



## OPEN ACCESS

## EDITED BY

Chuan-Zhou Liu,  
Institute of Geology and Geophysics  
(CAS), China

## REVIEWED BY

Lin Ma,  
Guangzhou Institute of Geochemistry  
(CAS), China  
Junpeng Wang,  
China University of Geosciences  
Wuhan, China

## \*CORRESPONDENCE

Yuanku Meng,  
ykmeng@foxmail.com

## SPECIALTY SECTION

This article was submitted to Petrology,  
a section of the journal  
Frontiers in Earth Science

RECEIVED 27 June 2022

ACCEPTED 15 August 2022

PUBLISHED 07 September 2022

## CITATION

Wang Q, Meng Y, Wei Y, Jiang L, Wang Z  
and Mao G (2022), Identification of the  
early cretaceous granitic pluton and  
tectonic implications in the middle  
gangdese belt, southern tibet.  
*Front. Earth Sci.* 10:979313.  
doi: 10.3389/feart.2022.979313

## COPYRIGHT

© 2022 Wang, Meng, Wei, Jiang, Wang  
and Mao. This is an open-access article  
distributed under the terms of the  
[Creative Commons Attribution License  
\(CC BY\)](https://creativecommons.org/licenses/by/4.0/). The use, distribution or  
reproduction in other forums is  
permitted, provided the original  
author(s) and the copyright owner(s) are  
credited and that the original  
publication in this journal is cited, in  
accordance with accepted academic  
practice. No use, distribution or  
reproduction is permitted which does  
not comply with these terms.

# Identification of the early cretaceous granitic pluton and tectonic implications in the middle gangdese belt, southern tibet

Qingling Wang<sup>1</sup>, Yuanku Meng<sup>1,2\*</sup>, Youqing Wei<sup>1</sup>, Li Jiang<sup>1</sup>,  
Zhenzhen Wang<sup>1</sup> and Guangzhou Mao<sup>1</sup>

<sup>1</sup>College of Earth Science and Engineering, Shandong University of Science and Technology, Qingdao, China, <sup>2</sup>Key Laboratory of Gold Mineralization Processes and Resource Utilization Subordinated to the Ministry of Land and Resources, Key Laboratory of Metallogenic Geological Process and Resources Utilization in Shandong Province, Jinan, China

The Gangdese magmatic belt of southern Tibet is an ideal place to study Neo-Tethyan subduction, continental crustal growth and reworking. However, there are still controversies with regard to the evolution of the Neo-Tethys Ocean, the magma source and the detailed diagenetic processes of igneous rocks in the Gangdese belt. The Early Cretaceous magmatic exposures are sporadic in the Gangdese magmatic belt. Thus the finding of the new exposure is key to understanding the scenarios of the Neo-Tethys Ocean and geological background of southern Tibet during the Early Cretaceous. In this contribution, we undertook systematic geochronology, whole-rock geochemistry and zircon Lu-Hf isotopic studies on a newly identified granitic pluton in the middle Gangdese belt (Quesang area), southern Tibet. The results show that zircon U-Pb dating of three representative samples yielded a weighted age of  $120 \pm 1.4$  Ma,  $117.3 \pm 2.5$  Ma and  $114.0 \pm 1.3$  Ma, respectively, which indicate the emplacement and crystallization age belonging to the Aptian stage of the Early Cretaceous in response to the northward subduction of the Neo-Tethyan oceanic lithosphere beneath the Lhasa terrane. *In situ* zircon Lu-Hf isotopic analyses indicate that  $\epsilon_{\text{Hf}}(t)$  values of the studied granitic pluton are predominantly positive ranging from 7.2 to 11.4, and one zircon shows negative  $\epsilon_{\text{Hf}}(t)$  value ( $-6.26$ ), implying that a small amount of ancient continental crustal materials might have participated in the magma evolution. Geochemically, the granite samples are enriched in large ion lithophile elements (LILE) and light rare earth elements (LREE), but depleted in heavy rare earth elements (HREE), indicating arc-type geochemical characteristics or subduction-related tectonic setting. In addition, combined with mineral assemblages, zircon Lu-Hf isotopic features and low molar  $\text{Al}_2\text{O}_3/(\text{CaO}+\text{Na}_2\text{O}+\text{K}_2\text{O})$  (A/CNK) ratios of 0.91–1.10, the studied samples show a close affinity with I-type granites. Moreover, zircon oxygen fugacity results show that  $\text{Ce}^{4+}/\text{Ce}^{3+}$  values range from 185 to 12, with a mean value of 78, indicating a low oxygen fugacity setting similar to the Chile ore-barren granitic plutons. In combination with published data, we argue that the Gangdese magmatic belt may have developed continuous magmatism (145–105 Ma),

and the notion of magmatic lull might deserve more consideration during the Early Cretaceous. In this study, the Early Cretaceous granitic pluton might be the result of the northward subduction of Neo-Tethys oceanic lithosphere beneath the Lhasa terrane at a normal angle.

#### KEYWORDS

zircon U-Pb-Hf isotopes, the Early Cretaceous, Gangdese magmatic belt, southern Tibet, Neo-Tethys Ocean

## 1 Introduction

Granites are widely generated in the whole processes of crustal formation and destruction/reworking and the evolution of orogenic belts, which is one of the most representative objects to delineate these dynamic scenarios (e.g., Wang T. et al., 2017). The southern Tibet is an ideal natural laboratory to explore the formation of various granites, growth and reworking of the continental crust (e.g., Yin and Harrison, 2000; Chung et al., 2005; Ma et al., 2017; Zhu et al., 2019; Ji et al., 2020; Zhang Y. Z. et al., 2021). The Gangdese magmatic belt, located in the southernmost part of the Lhasa terrane, is mainly composed of granitic rocks and volcanic-sedimentary sequences, with minor mafic assemblages (e.g., Scharer et al., 1984; Le and Cronin, 1988; Chung et al., 2003; Hou et al., 2004; Mo et al., 2007; Zhu et al., 2011, 2012; Zhang et al., 2012; Wang et al., 2013). Furthermore, the Gangdese belt is also an ideal place for unraveling the evolution of the Neo-Tethyan oceanic lithosphere and petrogenesis of arc-type magma (such as differentiation, evolution and metallogeny) (Xu et al., 2019). In the generation processes of arc magmatism, the dehydration and partial melting of subduction slab can significantly affect physical-chemical properties of the upper mantle wedge and lead to diversities of magmatic rocks in the convergent margin (Pearce et al., 2005).

Previous studies have shown that the formation of the Gangdese arc is related to the subduction of the Neo-Tethyan oceanic slab (e.g., Yin and Harrison, 2000; Ji et al., 2009a). Therefore, the magmatism of the Late Triassic to Latest Jurassic (230–145 Ma) in the Gangdese belt is generally related to the northward subduction of the Neo-Tethys Ocean beneath the Lhasa terrane (e.g., Chu et al., 2006; Ji et al., 2009a, b; Wang et al., 2016; Meng et al., 2016; Ma et al., 2018, 2020; Wang et al., 2020; Li et al., 2021). However, some researchers argue that the pre-Cretaceous magmatic activities might be the products of the southward subduction of the Bangong-Nujiang oceanic lithosphere in the Gangdese belt, southern Tibet (e.g., Zhu et al., 2011; Li et al., 2018). According to the characteristics of magmatic activities, four magmatic flare-ups are identified in the Gangdese magmatic belt, including the Late Triassic-Jurassic (230–152 Ma), Cretaceous (109–80 Ma), Palaeocene-Eocene (65–38 Ma), and Oligocene-Miocene (33–13 Ma) (Ji et al., 2009b; Meng

et al., 2016, 2018, 2020, 2021; Wang et al., 2016; Ma L. et al., 2019; Zhang Z. M. et al., 2019, 2020; Zhang Y. Z. et al., 2021). Increasing recognitions reveal that the magmatism of Gangdese belt is relatively weak during the earliest Early Cretaceous to late Early Cretaceous (e.g., Ji et al., 2009a; Zhu et al., 2011). Some invocers deemed that there is a magmatic lull in the Gangdese belt during the Early Cretaceous (e.g., Zhang et al., 2004; Kapp et al., 2007; Wen et al., 2008a, b), which is associated with flatten subduction of the Neo-Tethys oceanic lithosphere beneath the Lhasa terrane. This consensus is well supported by the geochronological framework of the Gangdese magmatic belt. Some scholars refuted this idea and proposed that there is no real magmatic lull in the Gangdese magmatic belt (e.g., Zhu et al., 2009a; Wang et al., 2013). Furthermore, Wu et al. (2010) conducted systemically studies on the sedimentary sequences of the fore-arc flysch of the Xigaze Group, and concluded that the Early Cretaceous might develop extensive magmatism (130–100 Ma) as suggested by the Early Cretaceous detrital zircon clusters derivation from the Gangdese magmatic belt, southern Tibet. There are many different arguments with regard to the geodynamic mechanism during this period, including the Neo-Tethyan subduction at a low angle (flatten slab) (Coulon et al., 1986; Ding et al., 2003; Kapp et al., 2003, 2005; Leier et al., 2007), and the rollback model of the Neo-Tethys Ocean (Zeng et al., 2017; Dai et al., 2021) or high-angle oblique subduction (Wang et al., 2013). Therefore, understanding the geochemical characteristics and formation processes of the Early Cretaceous arc-type magmatic rocks can provide new clues to evaluate the evolution of the Neo-Tethyan subduction and tectonic setting of southern Tibet. Moreover, previous studies have shown that the abnormality of the multivalent elements U, Ce, and Eu and the  $Ce^{4+}/Ce^{3+}$  ratios in zircon can be used to reflect the parent magma's oxygen fugacity (e.g., Ballard et al., 2002; Trail et al., 2012; Zhang et al., 2017; Zhang L. P. et al., 2021), which can further estimate the potential for mineralization. The evaluation of metallogenic potential of the Cretaceous subduction-related magmatic rocks is of great significance for mineral exploration in the Gangdese magmatic belt (Zhang L. P. et al., 2021). In this contribution, we firstly report an Early Cretaceous granitic pluton in the middle Gangdese magmatic belt of southern Tibet near Lhasa city. On the basis of detailed field and

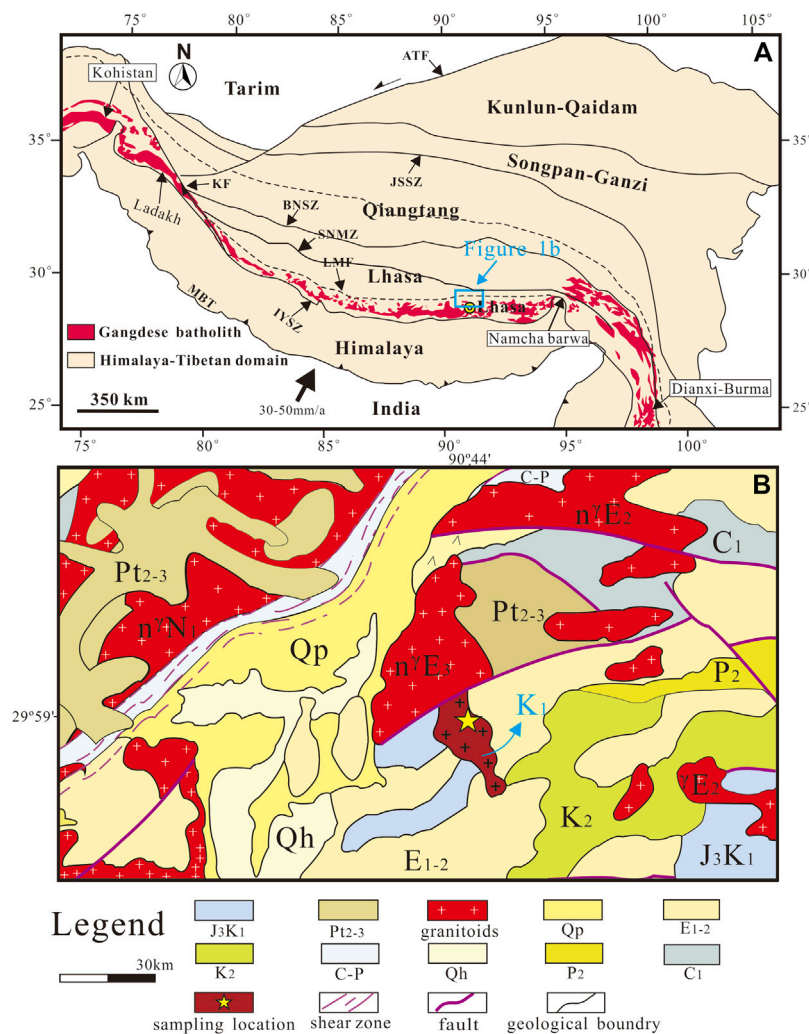


**FIGURE 1**

(A) Simplified tectonic framework of the Himalayan-Tibetan plateau (after Yin and Harrison, 2000; Zhu et al., 2011; Meng et al., 2021). (B) Regional geological map and sampling location (after 1:150,000 geological map of the Qinghai-Tibet Plateau and its adjacent areas)  $J_3K_1$ = Upper Jurassic-lower Cretaceous clastic rocks;  $E_{1-2}$ = Paleocene-Eocene mudstone/siltstone;  $K_2$ = Upper Cretaceous clastic/depositional rocks, limestone;  $Pt_{2-3}$  = Meso-Neo Proterozoic phyllite; Qh, Holocene sediments; Qp = Pleistocene clay, gravel;  $P_2$ = Middle Permian clastic-volcanic rocks.; CP= Carboniferous- Permian limestone;  $C_1$ = Lower Carboniferous limestone. Abbreviations: MBT, Main boundary thrust; IYSZ, Indus-YarlungZangbo suture zone; LMF, Luobadui-Mila Mountain fault; KF, Karakoram fault; BNSZ, Bangong-Nujiang suture zone; JSSZ, Jinshajiang suture zone; ATF, Altn Tagh fault; SNMZ, ShiquanRiver-NamTso Melange Zone.

petrographic observations, zircon U-Pb dating, Lu-Hf isotopes, whole-rock major and trace geochemical data and TIMA surface scanning analyses are provided to determine the formational age and geochemical characteristics of the granitic pluton, and reveal the magma source, evolution and geodynamic mechanism. Additionally, we calculated the oxygen fugacity of zircon and further discussed the ore-bearing property and potential of the granitic pluton. Our study further improves the geochronological framework of the Gangdese magmatic belt in southern Tibet, and contributes to

the deep understanding of the Early Cretaceous arc-type magmatism.

## 2 Geological setting and petrological features

The Himalayan-Tibetan Plateau is divided into five segments from north to south, Kunlun-Qilian, Songpan-Ganzi, Qiangtang, Lhasa and the Himalayan terranes (e.g., Yin and Harrison, 2000;

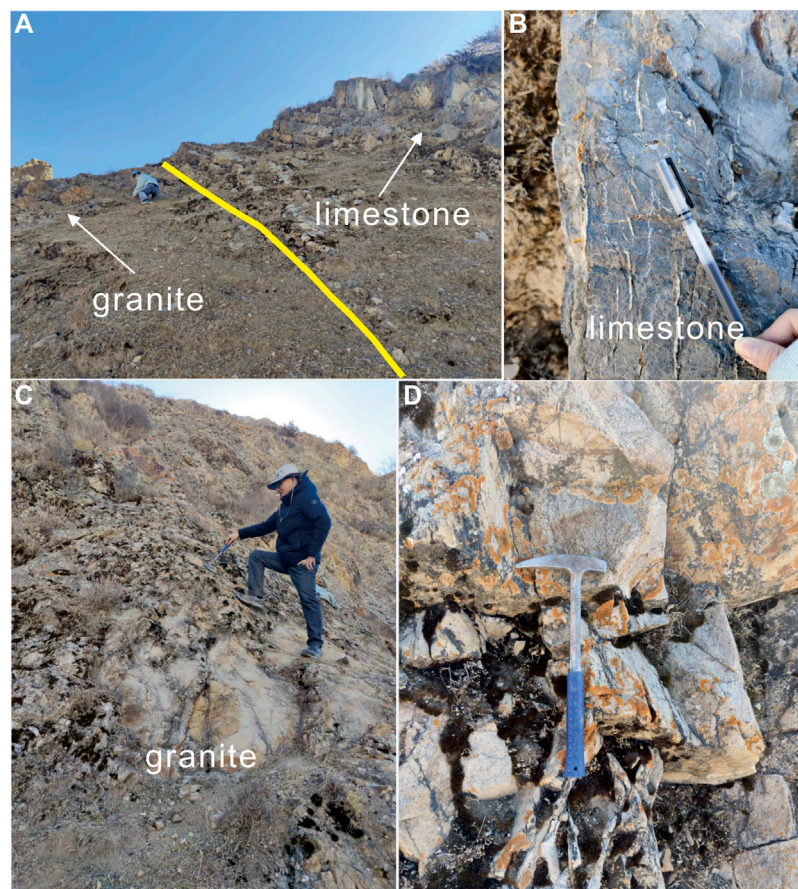


**FIGURE 2**  
Field exposures of the studied granitic pluton.

Kapp and DeCelles, 2019; Zhang L. P. et al., 2021), which are separated by the Indus-YarlungZangbo suture zone (IYZSZ), the Bangong-Nujiang suture zone (BNSZ), and the Jinshajiang suture zone (JSSZ), respectively (Figure 1A) (Yin and Harrison, 2000; Meng et al., 2019; Zhang L. P. et al., 2021). The Lhasa terrane is a tectono-magmatic belt extending nearly east-west, about 2,500 km in length and 150–300 km in width (e.g., Mo et al., 2008, 2009). According to the differences of granitoid rock types and isotopic features in the Lhasa terrane, Chu et al. (2006) and Wen et al. (2008b) divided it into two sub-terrane, Gangdese magmatic belt (mainly I-type granite) and northern granitic belt (mainly S-type granite). Based on the Hf isotopic mapping, Zhu et al., (2009a, 2011, 2013) and Hou et al. (2015) further divided the Lhasa terrane into northern Lhasa, central Lhasa and southern Lhasa sub-terrane by the Shiquan River-NamTso Melange Zone (SNMZ) and Luobadui-Mila Mountain fault (LMF), respectively. Tectonically, the Gangdese magmatic belt located in the southernmost part of the Lhasa terrane (Zhu et al., 2011), adjacent to the IYZSZ,

documenting the subduction history of the Neo-Tethys Ocean and the magmatism of Indo-Asia collision (e.g., Yin and Harrison, 2000; Kapp and DeCelles, 2019). As mentioned above, the Gangdese belt mainly comprises Late Triassic to Neogene granitoid rocks and coeval volcano-sedimentary sequences (e.g., Debon et al., 1986; Harris et al., 1988; Mo et al., 2008, 2009; Ji et al., 2009b). Previous studies reveal that the Cretaceous intrusive rocks in the Gangdese belt include gabbro, gabbro-diorite, diorite, tonalite, granodiorite, granite, etc (e.g., Yin and Harrison., 2000; Ji et al., 2009b; Ji et al., 2020; Zhang Y. Z. et al., 2021), which were related to the northward subduction of the Neo-Tethys oceanic lithosphere beneath the Lhasa terrane (e.g., Yin and Harrison., 2000; Meng et al., 2016, 2018,2020; Wang et al., 2016; Kapp and DeCelles, 2019; Ji et al., 2020; Zhang Y. Z. et al., 2021).

The study region lies in the middle segment of the Gangdese belt (Figure 1A), with a good transportation nearby Lhasa city. Previous geological mapping implies that the studied granitic pluton belongs to Late Paleogene granites. The detailed sampling

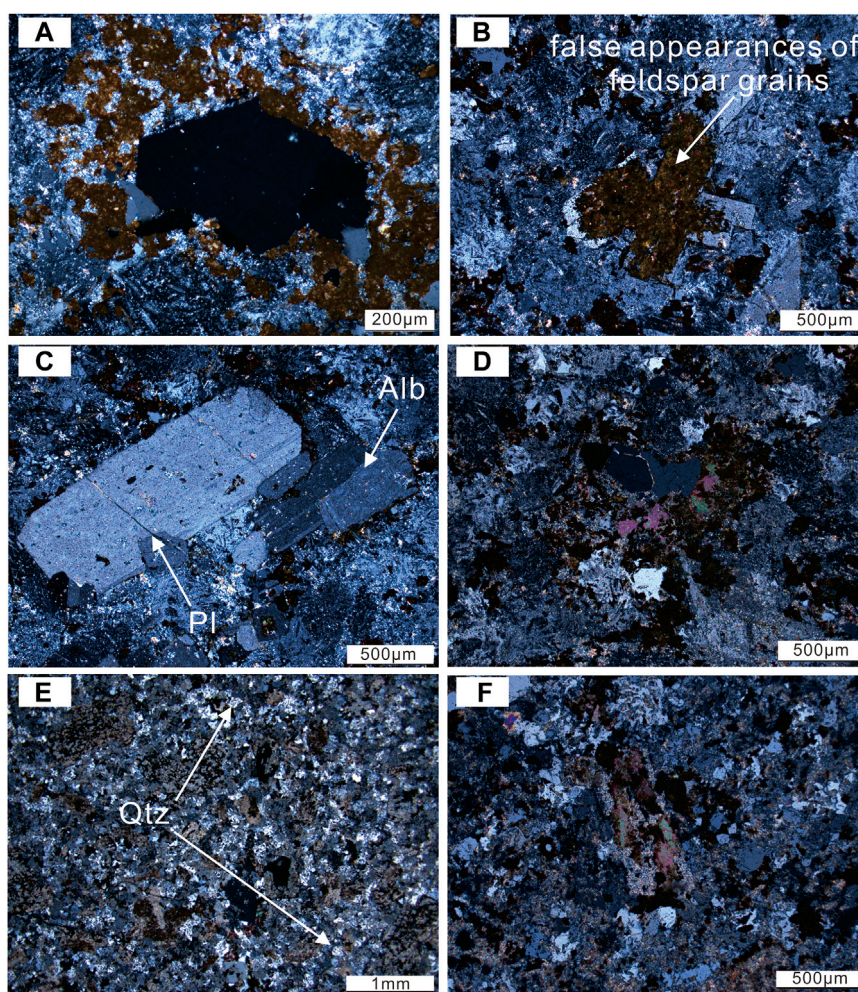


**FIGURE 3**

Microtextonic textures and thin-section photomicrographs of the newly identified granitic pluton. (A–D) belong to QSC01, (E,F) belong to QSC02. Qtz, quartz, Alb, albite, Pl, Plagioclase.

location is nearby the Quesang village, about 60 km of Lhasa city to northwest (Figure 1B). The newly identified pluton shows irregular distributions, intruding into the Late Jurassic limestone of the Duodigou Formation (Figures 2A–C), and the field relationship with the Eocene strata is unconformity contact. The GPS positions of the sampling points are at N29°59′42″, E90°44′38″ and N29°59′33″, and E90°44′38″, respectively. The granitic pluton experienced intermediate-degree weathering (Figure 2D), but the recovered rocks in this study are relatively fresh. A total of twenty-two representative samples were taken to carry out detailed petrology, geochemistry and mineral observations in this study.

The newly identified granitic pluton is light grey with typical massive textures, and all samples show medium to fine-grained textures and similar mineral assemblages. The thin section analyses indicate that the studied samples experienced

significant chemical weathering (Figures 2A–F). The pluton mainly consists of quartz and albite (Figures 3A–F), and furthermore, the false appearances of feldspar grains (Figure 3B) could be observed as suggested by tabular laths. Thus, a refined TIMA analyses was performed to identify the mineral compositions of the newly identified granitic pluton. Combined with the TIMA surface scanning results, abundant sericite assemblages are found in the newly identified granite pluton which are the products of the sericitization of plagioclase grains (e.g., albite). In addition, a weak kaolinization phenomenon suggests the presence of K-feldspar grains. Rutile, zircon and apatite can also be observed in Figures 4A–F. As a common accessory mineral within the magmatic rocks, zircon is widely used to determine the crystallization ages of magmatic rocks, and can be used to estimate the magma temperature and oxygen fugacity (Ballard et al., 2002; Ferry and

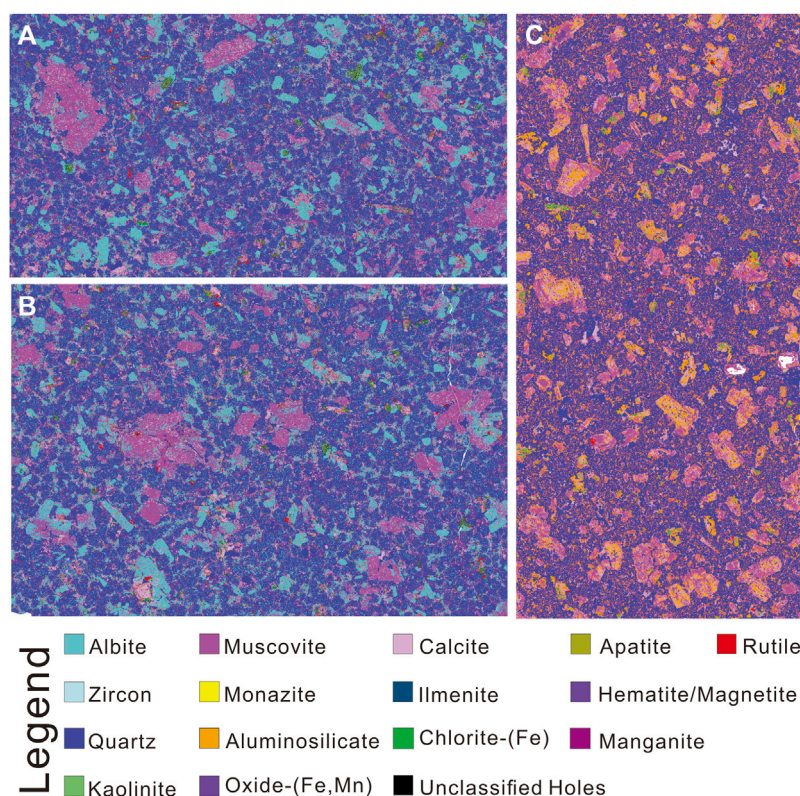


**FIGURE 4**  
TIMA results of the newly identified granitic pluton.

Watson, 2007; Zhang et al., 2017; Zhang L. P. et al., 2021), which can further evaluate the mineralization potential of intrusions.

The granitic sample QSC01 (Figures 3A–D) mainly comprise of plagioclase, K-feldspar and albite (50%–60%), quartz (20%–30%), sericite (10%–15%), calcite (~5%) and accessory minerals, such as magnetite (<1%) and chlorite (<1%). The granitic sample QSC02 (Figures 3E,F) mainly comprises of quartz (20%–35%), plagioclase, K-feldspar and albite (50%–55%), sericite (10%–15%), calcite (~5%), with accessory minerals magnetite chlorite and aluminosilicate (<5%). And they also have a small quantity of unclassified minerals (<3%).

### 3 Analytical methods

#### 3.1 Zircon U-Pb geochronology analyses

In order to determine the crystallization age of the Quesang granitic pluton, three representative samples (QSC01-1, QSC02-1 and YK3-3) were selected for laser-ablation-inductively coupled plasma-mass spectrometry (LA-ICP-MS) *in situ* zircon U-Pb isotopic dating analyses. Zircon separation and

cathode luminescence images (CL) were undertaken at the Beijing ZhongKeKuangYan Geoanalysis Laboratory Co., Ltd (Beijing, China). Zircon LA-ICP-MS U-Pb dating was completed at the Shandong university of science and technology (Qingdao, China) and State Key Laboratory of Continental Dynamics (Xi'an, China), respectively. The laser ablation spot diameter is 32  $\mu\text{m}$  and the carrier gas is Helium. Zircon 91500 and glass NIST610 are external standards for U-Pb dating calibration. The software ICPMSDataCal 9.0 was used for off-line data processing completed. The detailed analytical methods and procedures are described by Zong et al. (2017). The zircon U-Pb dating results are listed in Supplementary Table S1.

#### 3.2 Zircon Lu-Hf isotopes

Two representative samples (QSC01-1, QSC02-1) were selected for *in situ* zircon Lu-Hf isotopic analyses. *In situ* zircon Lu-Hf isotope analyses were performed at the Wuhan Sample Solution Analytical Technology Co., Ltd. By using Neptune Plus MC-ICP-MS (Thermo Fisher Scientific,



**FIGURE 5**  
Representative zircon cathodoluminescence (CL) images (red circles for U-Pb dating field, yellow circles for Lu-Hf analytical domain).

Germany), and combined with a Geolas HD excimer ArF laser ablation system. Helium was used as the carrier gas of denudation material in the experiment. The detailed analytical methods and procedures are described by [Hu et al. \(2012\)](#). Zircon Lu-Hf isotopic analyses were performed at the same location as the *in-situ* U-Pb dating site, and the measured Hf values are consistent with the recommended values. The zircon Lu-Hf isotope data are listed in [Supplementary Table S2](#).

### 3.3 Major and trace whole-rock elements

In order to determine the geochemical features of the newly identified granitic pluton, eight representative samples (QSC01-4~7, QSC01-9~10 and QSC02-4~5) were selected for whole-rock major and trace elements analyses. The major elements data were performed at the laboratory of Shandong University of Science and Technology and Wuhan Sample Solution Analytical Technology Co., Ltd. Using X-ray fluorescence (XRF) (Primus II, Rigaku, Japan), respectively. Whole-rock trace element composition analyses were performed at the Wuhan Sample Solution Analytical Technology Co., Ltd. Using Agilent 7700e ICP-MS. The major and trace whole-rock data are presented in [Supplementary Table S3](#).

### 3.4 TIMA surface scanning

Three samples (QSC01-2, QSC01-3 and QSC02-2) were selected for TESCAN Integrated Mineral Analyzer (TIMA)

analyses. Mineral semi-quantitative scanning and measurements were performed at the Nanjing Hongchuang exploration technology service Co., Ltd. using TESCAN integrated mineral analyzer (TIMA). TIMA technique can detect 500 nm mineral sizes and has the ability of automatic identification mineral compositions. TIMA was performed at 25 kV working voltage with a spot size of 110 nm, a working distance of ca. 15 mm. Analytical zones had dimensions of 10 mm × 10 mm in the thin sections. Detailed analytical processes and principles are shown in [Hrstka et al. \(2018\)](#). The TIMA surface scanning data are presented in [Supplementary Table S4](#).

## 4 Analytical results

### 4.1 Zircon U-Pb dating results

The representative zircon CL images are shown in [Figure 5](#). It reveals that zircons in this study area are predominately prismatic morphologies. These zircon grains are approximately 100–400 μm in length with the ratios of length to width are about 1:1 to 4:1. Zircons are characterized by clear oscillatory textures with high ratios of Th/U values (>0.4), indicating an igneous origin ([Hoskin and Schaltegger, 2003](#)). In addition, some zircon grains are characterized by core-rim textures. The Concordia diagram and weighted average age of zircon dating are shown in [Figure 6](#). As shown in [Figures 6A,B](#), 30 points were assayed for the sample QSC01, the valid points are 24 (with six dating

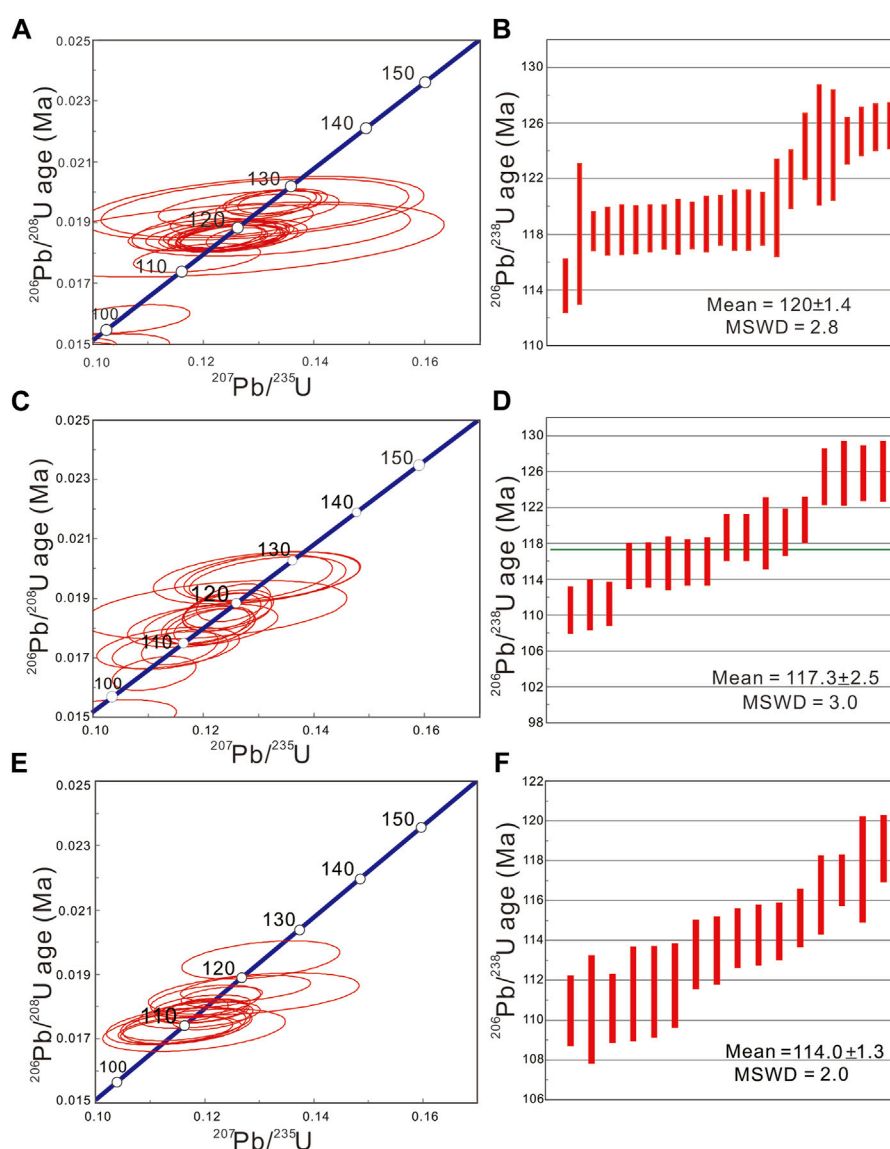


**FIGURE 6**  
LA-ICP-MS zircon U-Pb Concordia diagrams for the granitic pluton.

points excluded), with a weighted average age of  $120 \pm 1.4$  Ma (MSWD = 2.8). Moreover, there is an inherited zircon grain with an age of 349 Ma (lath shaped, and Th/U = 0.4). The contents of Th and U elements range from 40.6310 to 668.06 ppm, 44.49 to 610.6710 ppm, respectively. In [Figures 6C,D](#), 20 points were assayed for the sample QSC02, and the valid points are 17 (with three dating points excluded), with a weighted average age of  $117.3 \pm 2.5$  Ma (MSWD = 3.0), and the contents of Th and U elements varying from 65.85 to 1,276.65 ppm and 79.25–776.76 ppm, respectively. As shown in [Figures 6E,F](#), the valid points are 16 of the sample YK3-3, with a weighted average age of  $114.0 \pm 1.3$  Ma (MSWD = 2.0),

and the contents of Th and U elements vary from 71.65 to 848.13 ppm and 87.87 to 1,009.66 ppm, respectively.

## 4.2 Zircon Lu-Hf isotopic results

A total of 30 *in-situ* zircon Lu-Hf analyses were performed on samples of the newly identified granitic pluton ([Figures 7A–D](#)). The  $\epsilon_{\text{Hf}}(t)$  values range from 7.2 to 11.4 (one point excluded,  $\epsilon_{\text{Hf}}(t)$  value =  $-6.26$ ), with a mean value of 9.7, and two-stage model ages ( $T_{\text{DM}2}$ ) vary from 442.7 to 704.9 Ma (one point model age = 1743.3 Ma), the  $T_{\text{DM}C}$  range from

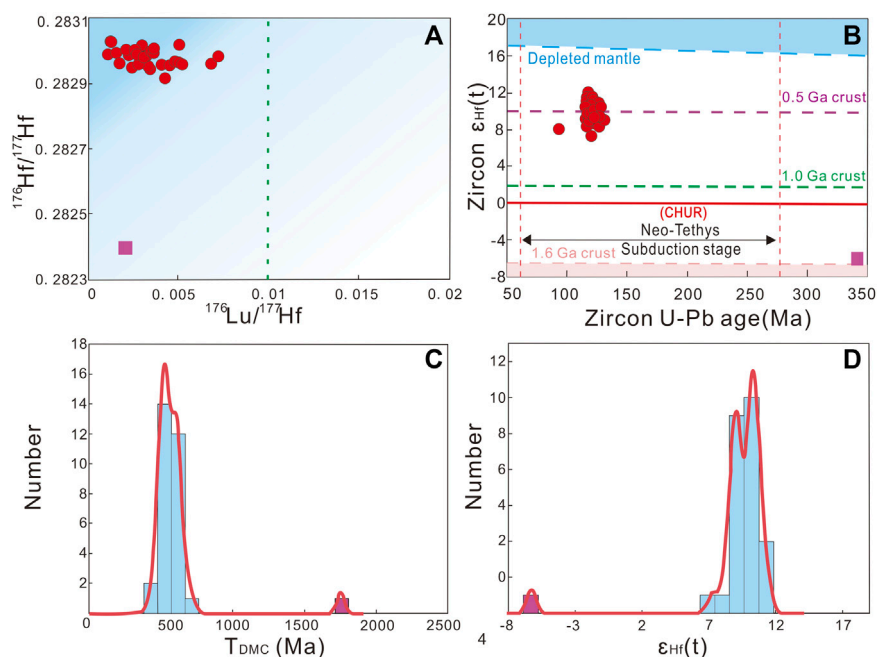


FIGURE 7

Zircon Lu-Hf isotopic results (A)  $^{176}\text{Lu}/^{177}\text{Hf}$  vs.  $^{176}\text{Hf}/^{177}\text{Hf}$  diagram. (B) Zircon U-Pb age vs.  $\epsilon_{\text{Hf}}(t)$  diagram. (C) Histogram of the model age ( $T_{\text{DMC}}$ ). (D) Histogram of  $\epsilon_{\text{Hf}}(t)$  values.

444.5 to 707.6 Ma (one point model age = 1751.7 Ma) (Figure 7C), with a mean value of 557.4 Ma. The  $^{176}\text{Hf}/^{177}\text{Hf}$  ratios are relatively high, ranging from 0.28292 to 0.28303. The values of  $^{176}\text{Lu}/^{177}\text{Hf}$  varies from 0.00112 to 0.00708 (mean value = 0.003536) (Figure 7A). Zircon Lu-Hf isotopic analyses show that the  $\epsilon_{\text{Hf}}(t)$  values predominantly are positive and only one inherited zircon shows negative  $\epsilon_{\text{Hf}}(t)$  values of -6.26 (Figure 7B). The ratios of  $^{176}\text{Lu}/^{177}\text{Hf}$  are all less than 0.002, indicating that there is almost no accumulation of radioactive Hf isotopes after zircon crystallization and post-magmatism.

## 4.3 Whole-rock geochemical results

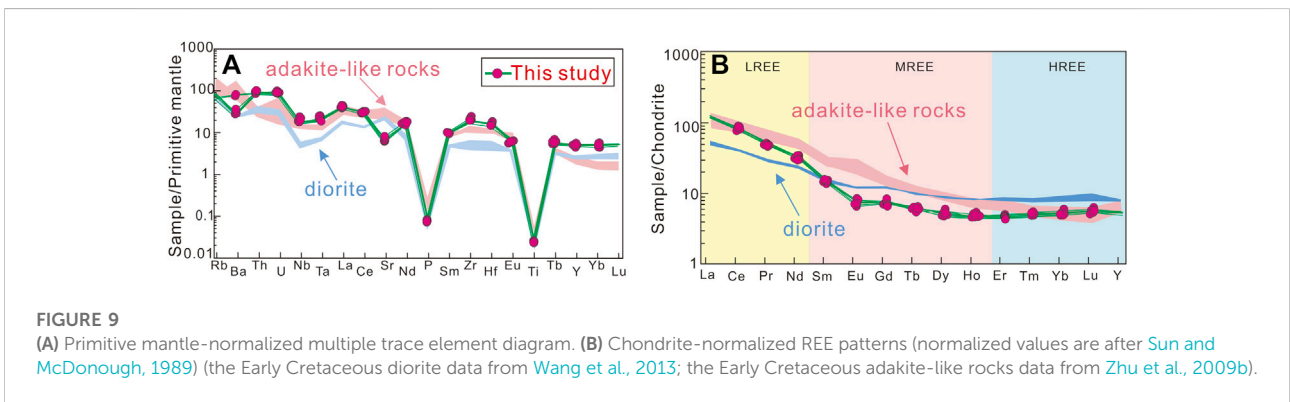
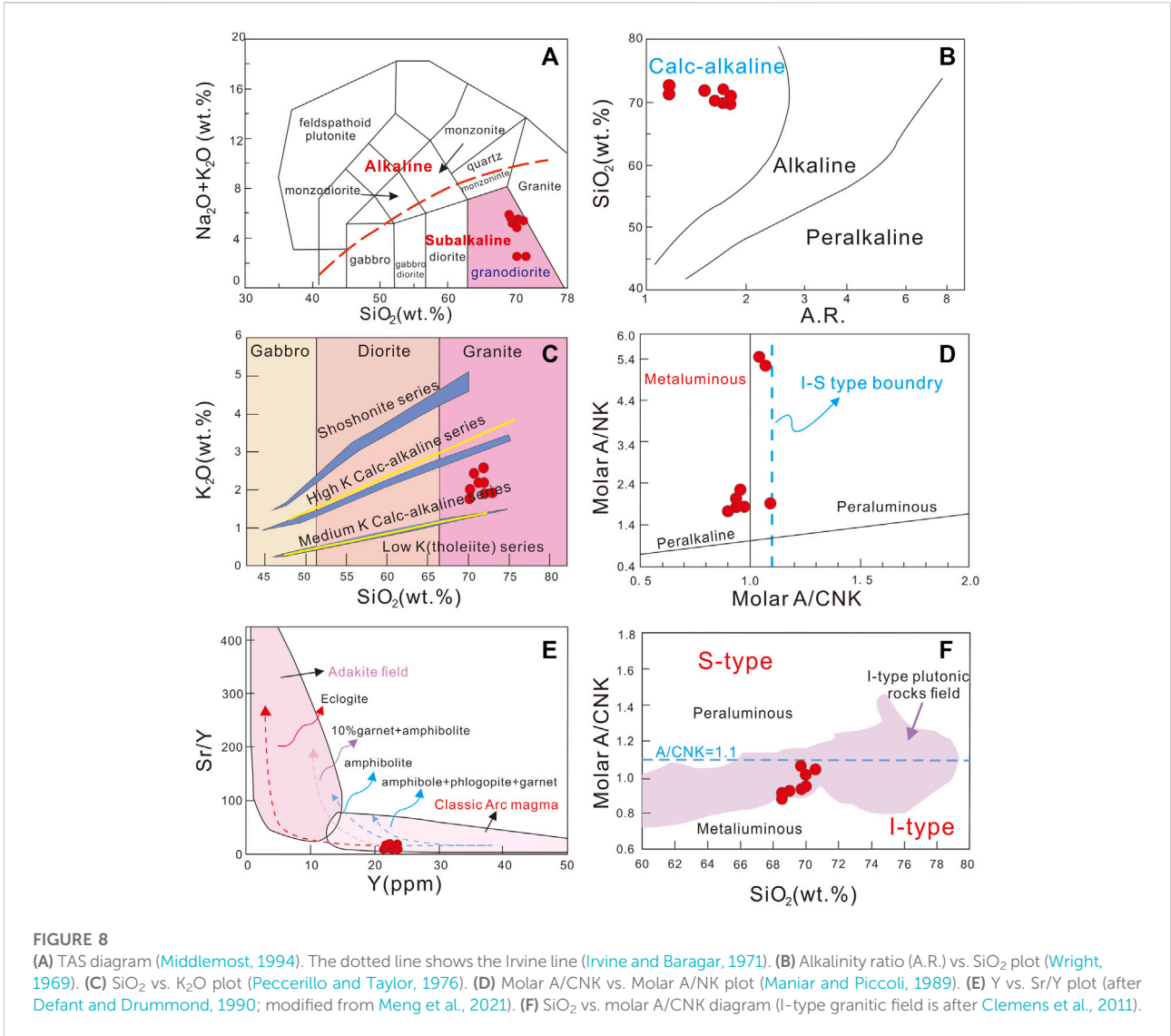
### 4.3.1 Major elements geochemical features

According to major element compositions and the division method of Irvine and Baragar (1971), the samples from the Early Cretaceous granitic pluton mainly plot in the range of subalkaline series, and plot within the granodiorite field (Figure 8A). In the  $(\text{Al}_2\text{O}_3 + \text{CaO} + \text{Na}_2\text{O} + \text{K}_2\text{O}) / (\text{Al}_2\text{O}_3 + \text{CaO} + \text{Na}_2\text{O} + \text{K}_2\text{O})$  (A.R.) vs.  $\text{SiO}_2$  diagram, the samples demonstrate calc-alkaline features (Figure 8B). Furthermore, according to the  $\text{SiO}_2$  vs.  $\text{K}_2\text{O}$  covariant diagram, the granodiorite in this study belongs to the medium K calc-alkaline series (Figure 8C).

The contents of  $\text{SiO}_2$  are relatively high, with a limited variation of 70wt% to 71.5wt%. The contents of  $\text{Na}_2\text{O}$  and  $\text{K}_2\text{O}$  vary from 0.56wt% to 3.75wt%, 1.73 to 2.78wt%, respectively. The ratios of  $\text{Na}_2\text{O}/\text{K}_2\text{O}$  range from 1.1 to 2.1, but one sample has low ratio of 0.3, with a mean value of 1.68, showing sodium-rich features. The contents of  $\text{MgO}$  and  $\text{FeO}$  are 0.32wt% to 0.38wt% and 2.7wt% to 3.2wt%. The contents of  $\text{TiO}_2$  and  $\text{MnO}$  are lower than 0.5wt% and 0.1wt%. The contents of  $\text{Al}_2\text{O}_3$  are relatively high, ranging from 15.4wt% to 15.7wt%. The ratios of molar  $\text{Al}_2\text{O}_3/\text{CaO} + \text{Na}_2\text{O} + \text{K}_2\text{O}$  (A/CNK) varied from 0.95 to 1.1. Detailed petrogenetic classifications and descriptions are discussed below.

### 4.3.2 Trace element geochemical features

The trace and rare earth elements (REE) distribution patterns of the granodiorite in this study are shown in Figures 9A,B. On the whole, they are characterized by trace elements of arc-type magmatic rocks. The contents of Ni and Cr elements are relatively low, varying from 1.21 to 1.52 ppm and 1.44 to 2.36 ppm, respectively. The contents of Rb, Sr, Th, U, Pb elements range from 47.1 to 57.1 ppm, 119.56 to 156.62 ppm, 7.69 to 7.87 ppm, 1.82 to 1.96 ppm and 2.83 to 4.1 ppm, respectively. The total REE contents vary from 125 to 130 ppm, and the LREE/HREE ratios range from 3.09 to 3.24. In combination with  $(\text{La}/\text{Yb})_{\text{N}}$  values



(7.83–8.51), it reveals that LREE is enriched but HREE depleted in the newly identified granitic pluton (Figure 9B). The Sr/Y ratios are considerable low, about 5.3–7.0. Due to the distribution coefficient  $K_D$  (Sr) being far less than 1 (e.g., Wang et al., 2013), therefore, the fractional crystallization of hornblende caused the studied samples having higher Sr contents (ca. 119–157 ppm). The analyzed granodiorite samples have calculated zircon  $Ce^{4+}/Ce^{3+}$ , with ratios of 12–358 with an average of 83.35, and  $Ce/Nd$  values range from 2 to 22, with an average of 8.6. The detailed petrogenetic processes of the granitic pluton are described below.

## 5 Discussion

### 5.1 Geochronology and classification

#### 5.1.1 Geochronology

According to the published data, the distribution of the Early Cretaceous magmatic activities mainly occurred in the southernmost margin of the Lhasa terrane (e.g., Hoskin and Schaltegger, 2003; Wen et al., 2008a). However, the Early Cretaceous magmatic rocks are poorly constrained. Wang et al. (2013) reported a Langxian diorite pluton that formed in the Early Cretaceous with depleted zircon Hf isotopic compositions ( $\epsilon_{Hf}(t)$  values = 3.4–6.9), indicating a juvenile crustal feature. Wang et al. (2020) reported the Early Cretaceous granitic gneisses characterized by arc-type features, and depleted Hf isotopic compositions ( $\epsilon_{Hf}(t)$  = 10.9–15.1) in Langxian area. In addition, the sedimentary rocks of the Xigaze fore-arc basin and the YarlungZangbo River sediments both contain a large amount of the Early Cretaceous detrital zircons characterized by depleted Hf isotopic compositions, indicating that the Early Cretaceous detrital zircons were probably derived from the Gangdese magmatic belt (e.g., Liang et al., 2008; Wu et al., 2010). The above studies indicate that the Early Cretaceous magmatism of the Gangdese magmatic belt was probably widespread in southern Tibet.

Published geochronological and petrological data indicate that large-scale intrusions and magma reservoirs were formed by multiple-pulse emplacement and incremental assembly (Coleman et al., 2004; Glazner et al., 2004; Annen, 2011). Ma et al. (2020) proposed that most of the granitic plutons belong to composite plutons, which were the products of multiple batches of magma addition. Through detailed studies on a late Cretaceous granitic pluton in Namling area (86.5 to 94.63 Ma), Meng et al. (2020) proposed that it experienced a pulse diagenesis process (last for 8 million years). Furthermore, Meng et al. (2022) deemed that a granitic pluton generally was a process of multiple cumulative assemblies rather than directly formed by crystallization diagenesis.

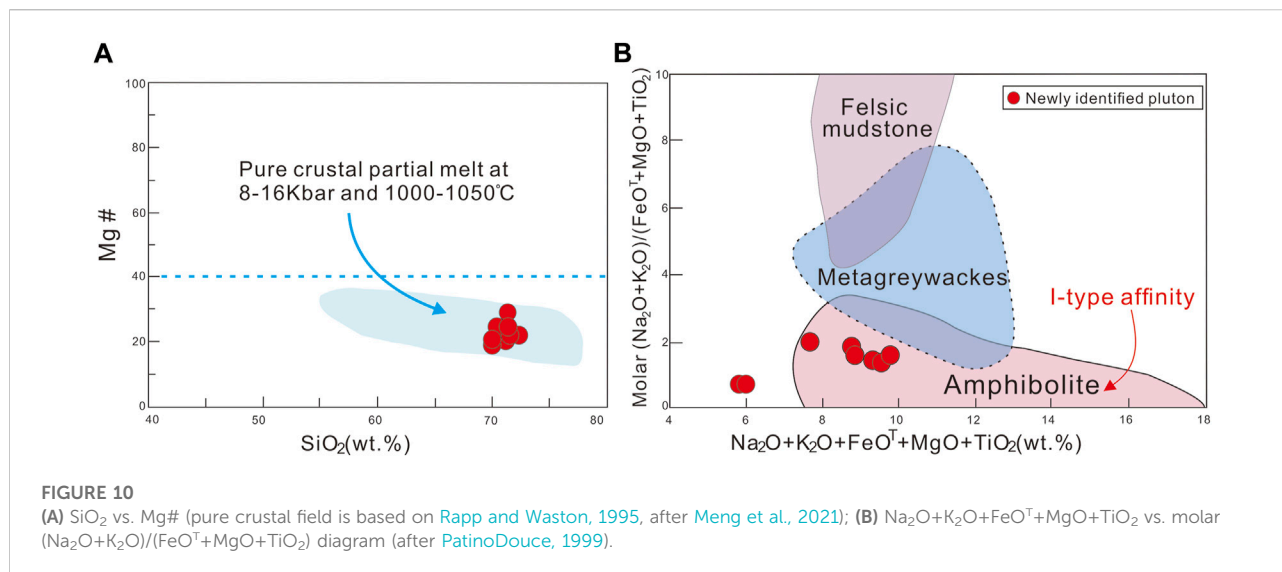
The zircon weighted average ages demonstrate that the granitic pluton might experience an incremental assembly

process (Figures 6B,D,F) from 114 Ma to 120 Ma (but magma emplacement peak at ca. 120 Ma), indicating that emplacement and crystallization timing belong to the Aptian stage of the Early Cretaceous rather than the Oligocene (Late Paleogene) as previous considered. Our study firstly suggests that the Early Cretaceous magmatism occurred in the middle Gangdese belt nearby the Lhasa area.

#### 5.1.2 Classification

The granites can be classified into M, I, A and S types according to their petrogenetic background and magma sources (e.g., Chappell and White, 1974; Wu et al., 2007, 2017). Generally, A-type granites are characterized by low  $H_2O$ , alkali compositions and produced in the intraplate setting (e.g., Loiselle and Wones., 1979; Liu et al., 2022). M-type granites are associated with mantle magma fractionation or multiple-evolved remnants of mafic suites (e.g., Pitcher, 1983; Meng et al., 2021). I-type granites generally originate from partial melting of igneous or metamorphic igneous rocks, and mantle contributions play an important role in the formation of I-type granities (e.g., Castro, 2020; Li et al., 2021). S-type granites usually originate from partial melting of metamorphic sedimentary rocks or sedimentary rocks, with relative low zircon saturation temperatures (e.g., Wang L.X. et al., 2017; Zhang H. L. et al., 2019; Meng et al., 2021). Compared with I-type granites, S-type granites are enriched in high aluminum minerals (such as muscovite, cordierite and garnet). Latest studies have concluded that granites have a complicated origin, and it has been proved that a small amount of sediments can participate in the formation of I-type granites (e.g., Li et al., 2022), resulting in granitic diversities and inhomogeneous of magma sources. Therefore, I- and S-type granites generally have gradual geochemical features using mineral and whole-rock geochemistry methods.

The depleted Hf isotopic compositions and young model ages rule out the possibility of S-type granites. It has been proved that S-type granites are characterized by enriched isotopic compositions and high  $K_2O/Na_2O$  ratios, which are not consistent with the granitic pluton in this study. According to zircon Lu-Hf isotope features, the source rocks of the newly identified granitic pluton are mainly originated from meta-igneous rocks with minor sedimentary components. Additionally, the geochemical discrimination diagram demonstrate that the molar A/CNK values are less than 1.1 (Figure 8D), showing arc-type geochemical features (Figure 8E) and the granodiorite samples fall into the range of metaluminous field, belonging to I-type granitic field (Figure 8F). Moreover, as shown in Figure 10B, the newly identified granite pluton plots in the



area of amphibolite compositions, indicating that the granite is originate from partial melting of the mafic lower crust, and corresponds to the composition of meta-igneous rocks consistent with I-type granites. In summary, the granite pluton in the study area belongs to I-type granites and the source rocks of the newly identified granite pluton are mainly originated from partial melting of the meta-igneous rocks with minor/insignificant sedimentary components.

## 5.2 Petrogenesis

### 5.2.1 Magmatic process

The Gangdese belt is a giant and composite magmatic belt, which contains a numerous of arc-type magmatic rocks associated with the subduction of the Neo-Tethyan oceanic slab before the Earliest Eocene (e.g., Ji et al., 2009a; Zhu et al., 2017). Zhao et al. (2021) proposed that under the setting of convergent plate margins, the oceanic slab subducting to a certain depth will dehydrate and metasomatize the overlying mantle wedge, resulting in partial melting of the mantle wedge to produce arc magmatism, subsequently the basic or intermediate-basic magmas generate arc-type intrusive-volcanic assemblages.

Nevertheless, magmatic rocks with arc-type features can be formed in different tectonic settings and scenarios (e.g., Ma et al., 2021). In case of the magma source contains rutile, ilmenite and other minerals which are enriched in high field strength elements (HFSE), and then the residual melts/magma will be depleted in HFSE, showing an arc-type feature (e.g., Zhang H. L. et al., 2019). Generally, the arc-type magmatic rocks are produced by three processes: 1) Partial melting of subducted slab (e.g., Defant and Drummond, 1990; Kay et al., 1993). 2) Partial melting of basic lower crust (e.g., Atherton and Petford, 1993). 3) Partial

melting of metasomatized mantle wedge (e.g., Atherton and Sanderson, 1985; Rogers and Hawkesworth, 1989; Sajona et al., 1996). Adakites were usually produced in the possibilities 1) and 2). Compared with the Early Cretaceous adakite-like rocks (Zhu et al., 2009b), the granitic pluton in the study area has low Sr/Y and  $(\text{La}/\text{Yb})_{\text{N}}$  ratios, and does not show the characteristics of adakitic rocks (Figure 9).

The newly identified granitic pluton in this study shows arc-type geochemical characteristics. Moreover, in the spider diagram of trace elements (Figure 9A), they are enriched in large ion lithophile elements (LILE), such as Rb, Ba, Th, U and LREE (La, Ce), but depleted in high field strength elements (HFSE) such as Nb, Ta, and Ti, reflecting a nature of arc-type magmatic rocks (Figure 9). Chen et al. (2021) considered that amphibole is the key mineral in terms of HFSE depletion in arc-type magmas. Based on trace element patterns and geochemical features, we deem that Nb-Ta depletion may result from amphibole differentiation (Meng et al., 2021). The rare earth elements of the granitic pluton have low differentiation with slightly negative Eu anomalies (Figure 9B), indicating that insignificant fractional crystallization of plagioclase occurred during the magmatic evolution. Additionally, the samples are enriched in Zr and Hf, which is corresponding to crustal affinity. Based on the variable whole-rock geochemical elements and depleted Lu-Hf isotopic compositions, we argue that the newly identified granite pluton derived from partial melting of mafic arc-type magmatic rocks.

### 5.2.2 Magma source and petrogenesis

The petrogenesis of the Early Cretaceous magmatism remains controversial due to sporadic distributions of the

magmatic rocks in the Gangdese belt. Harris et al. (1988) proposed that the basic magma of the Gangdese magmatic belt originated from the mantle with garnet residual. Then the basic magma formed intermediate-acid granites through fractional crystallization and crustal contamination. Furthermore, Meng et al. (2021) proposed two-stage petrogenetic dynamic processes, the first stage: northward subduction of the Neo-Tethyan oceanic lithosphere led to partial melting of the overlying asthenospheric mantle and forming mafic lower crust with a basaltic composition; in the second stage, juvenile mafic lower crustal materials experienced partial melting and then produced the granites in the Gangdese belt.

Ji et al. (2009b) deemed that the southern Gangdese is an intra-oceanic arc terrane, which was accreted to the southern margin of the Asian continent in the Late Permian. The fact is that most Mesozoic and Cenozoic magmatic rocks show depleted whole-rock Nd and zircon Hf isotopic compositions, indicating that they originate from the YarlungZangbo Neo-Tethys Oceanic crust and/or partial melting of juvenile crust or related to the mixing of mafic and felsic magma. In combination of published and newly obtained data, Ma X. X. et al. (2019) suggested that the southern Lhasa terrane is not a complete neof ormative terrane, but participated in the Tethys evolution and the crustal accretion as a micro-continent. Based on enriched Hf isotopic composition of the mafic rocks in the Daju area, Huang et al. (2020) proposed that the ancient lithospheric mantle materials may have existed in the lower part of the Gangdese area for a long time.

The SiO<sub>2</sub> contents of the newly identified granitic pluton are relatively high (70.14wt% to 72.18 wt%), indicating that the granitic pluton might be derived from partial melting of crustal materials or remnants of fractional crystallization of mantle derived magma. Compared with primitive mantle (Mg# > 70, Cr > 2,500 ppm, Ni > 1800 ppm) (McDonough, 2003), the granodiorite in this study has low Mg# values, Cr and Ni contents, suggesting that there is crystallization fractionation during the magma evolution process (Meng et al., 2021).

In the SiO<sub>2</sub>-Mg# diagram (Figure 10A), the granite samples fall within the range of pure crustal partial melt, and the studied granitic pluton has a lower Mg# values (16.8–26.9, mean value = 20.48) which indicates that the samples might be derived from pure crustal material with insignificant input of mantle-derived magma. The Lu-Hf isotopic compositions of the newly identified granitic pluton is depleted, which show the same evolutionary line as the reported Hf isotope of Mesozoic magmatic rocks in Gangdese belt, indicating that the magma source of the granitic pluton has the characteristics of depleted mantle-derived materials. The  $\epsilon_{\text{Hf}}(t)$  values range from 9 to 11, spanning 4 $\epsilon$  units, revealing that there is probably a minor heterogeneity in the magma source. The heterogeneity may be caused by two aspects, and one possibility is the addition of sediment, and the other may be a small amount of ancient materials (e.g., basements) participating in the magma evolution.

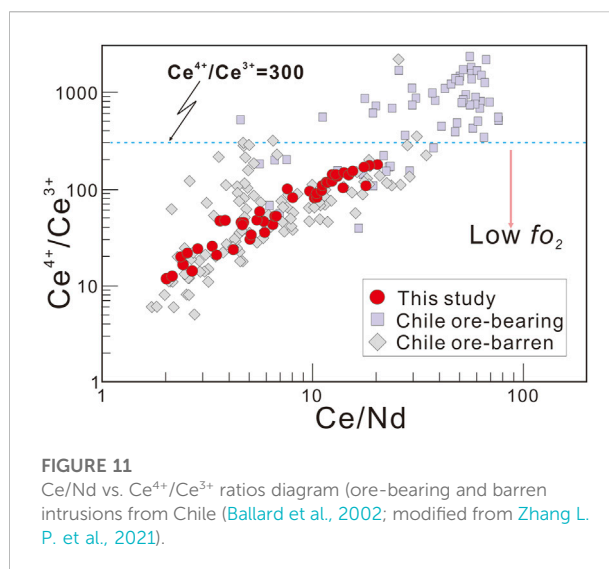


FIGURE 11  
Ce/Nd vs. Ce<sup>4+</sup>/Ce<sup>3+</sup> ratios diagram (ore-bearing and barren intrusions from Chile (Ballard et al., 2002; modified from Zhang L. P. et al., 2021).

In conclusion, the Gangdese magmatic belt is not a complete juvenile arc, and it is likely incorporating ancient basement materials or an ancient nucleus (Dong et al., 2010; Ma et al., 2016; Meng et al., 2022), which can well explain the generation of inherited zircons and depleted Hf isotopic compositions in this study (Figure 7B). According to the above, we argue that the newly identified granitic pluton may originate from partial melting of juvenile crust with arc-type characteristics, and a minority of ancient basement material participated in the formation of the granite during the evolution process.

### 5.2.3 Oxygen fugacity and metallogeny

Zircon Ce<sup>4+</sup>/Ce<sup>3+</sup> ratios are an effective tool for evaluating the oxygen fugacity of a magma chamber. Oxygen fugacity of magma is one of the most important factors constraining Cu and Au mineralization during the evolution process. Hou et al. (2015) proposed that the Cenozoic collision-related porphyry Cu deposits may be related to re-melting of the former subduction-related mafic arc, which implies that subduction-related magma may have already been enriched in and gathered ore-forming elements (Zhang L. P. et al., 2021). Several Late Cretaceous subduction-related deposits have been reported in the southern Gangdese magmatic belt, such as the Shuangbujiere skarn Cu-Au deposit dated at circa 92 Ma (Zhao et al., 2012; Huang et al., 2020), and the Kelu deposit dated at circa 92 Ma (Jiang et al., 2012; Huang et al., 2020). In contrast, the Early Cretaceous subduction-related deposits have not been found up to date.

As shown in Figure 11, zircons in this study have low Ce<sup>4+</sup>/Ce<sup>3+</sup> ratios (<300) (Supplementary Table S5), corresponding to a low magma oxygen fugacity. Previous studies have shown that Ce<sup>4+</sup>/Ce<sup>3+</sup> ratios have a wide range of variation (e.g., Ballard et al., 2002), and they will gradually increase with the intrusion ages

from ancient to juvenile, mafic to felsic, and are positively correlated with the Eu anomalies of zircons. Meaningfully, intrusions with porphyry copper mineralization are usually more than 300 of  $Ce^{4+}/Ce^{3+}$  and 0.4 of  $Eu/Eu^*$ . On the contrary, the intrusions without ore are less than the values which are similar to the Chile ore-barren granitoid rocks (Figure 11). This trend is determined by the correlation of oxygen fugacity, morphology and solubility of S (sulfur) in silicate magma (e.g., Cao et al., 2019; Wei et al., 2019; Wu and Wang, 2020). The low oxygen fugacity of the Early Cretaceous granitic pluton may have limited the extent of mineralization in the study area. Combined with previous studies, we argue that the metallogenic elements may gradually enriched during the subduction process from the Early Cretaceous to the Late Cretaceous.

### 5.3 Tectonic significance and geodynamic background

According to the characteristics of temporal and spatial distributions of the magmatic rocks, it is generally believed that the Early Cretaceous magmatism of the Gangdese magmatic belt is related to the northward subduction of the Neo-Tethyan oceanic slab beneath the Lhasa terrane (e.g., Ji et al., 2009a, b; Chen et al., 2014; Huang et al., 2017; Li et al., 2018). However, the details of the subduction-related scenarios are remain enigmatic. Distributions and exposures of the Early Cretaceous igneous rocks in the Gangdese belt are very limited. There are only few reports in Langxian and Quxu-Dazhuka and Zedong areas (Quidelleur et al., 1997; Ji et al., 2009a; Zhu et al., 2009b; Wang et al., 2013). Therefore, the limited available data of the Early Cretaceous magmatic rocks has resulted in the proposal of conflicting scenarios. Some scholars suggest that the magmatism in the Gangdese belt has a tectono-magmatic quiet period (e.g., Dai et al., 2021), which is related to the low-angle subduction or flatten-slab subduction of the Neo-Tethys oceanic lithosphere beneath the Lhasa terrane (e.g., Coulon et al., 1986; Kapp et al., 2003, 2005, 2007; Leier et al., 2007; Ding et al., 2003; Zhang et al., 2004; Wen et al., 2008a, b). However, abundant Early Cretaceous detrital zircons with depleted Hf isotopic compositions in the Xigaze fore-arc basin suggest that the Gangdese magmatic belt of southern Tibet might developed intense magmatism (Zhu et al., 2009; Wu et al., 2010; Meng et al., 2019; Meng et al., 2022). In addition, it has been proved that the Gangdese magmatic belt suffered from rapid uplift and denudation during the Late Cretaceous, making it difficult to retain the Early Cretaceous magmatic rocks, then the exhumated and eroded materials were transported into the Xigaze fore-arc basin (Ge et al., 2018; Meng et al., 2019, 2022). As a result, the Early Cretaceous granites are

only sporadically distributed in the Gangdese belt of southern Tibet. This indicates that the so-called tectono-magmatic quiet period might not exist in the Gangdese area during the Early Cretaceous. Generally, magmatic activities will be terminated once the slab subduction stop. There was continuous magmatism during the Early Cretaceous, hence the flatten-slab subduction model maybe unreliable. In addition, numerous studies have shown that low-angle slab subduction cannot form/generate arc-type magma or can only form adakites at the front edge of the subducted slab. Thus, the low-angle northward subduction model cannot explain the discovery of the Early Cretaceous magmatism in Gangdese magmatic belt (e.g., Ji et al., 2009a, b; Wen et al., 2008a; Zhu et al., 2009a, b; Wu et al., 2010). Therefore, Wang et al. (2013) proposed that the Neo-Tethyan Ocean was subducted at a steeper angle rather than a low angle flat subduction during the Early Cretaceous. Moreover, based on the study of the intermediate-basic dikes in the granites around the Gangdese belt in Lhasa city, Gao et al. (2017) concluded that the Early Cretaceous-early Late Cretaceous (130–85 Ma) was a period of oblique subduction of the Neo-Tethyan Ocean. Furthermore, Ji et al. (2009a) and Wu et al. (2010) proposed that the Neo-Tethys Ocean was in a stable oblique subduction during this period, and the angle of subducted slab gradually increase in the middle and late Early Cretaceous (Ji et al., 2009a; Zeng et al., 2017). In addition, Zeng et al. (2017) argued that there is a significant retreat/rollback of the Neo-Tethys oceanic lithosphere during the late Early Cretaceous (110–100 Ma), indicating that it is a normal subduction angle of the Neo-Tethys Ocean before the Early Cretaceous (>110 Ma). After studying various Early Cretaceous granites preserved in the Langxian complex in the eastern Gangdese belt, Li et al. (2021) deemed that the Neo-Tethys oceanic slab experienced a long period of subduction in the early stage (240–144 Ma), and subduction of the Neo-Tethyan Ocean might experienced a critical reorganization enabling the introduction of an increased amount of sediments and fluids into the subducting system and the modification of the mantle wedge in the Early Cretaceous (~120Ma). As mentioned above, the newly identified granitic pluton has arc-type characteristics (enriched in LILE and LREE, depleted in HFSE and HREE), indicating that they were formed in a subduction-related tectonic setting. Combined with previous studies, we argue that the northward subduction of the Neo-Tethys Ocean played a vital role in the generation of the arc-type magmas during the Early Cretaceous.

The variations in crustal thickness are essential for understanding tectonic and geodynamic process, especially for tracking the switch of tectonic settings, evolution and development of the lithosphere of planet during the geological time (Hu et al., 2017). The empirical formulas can be used to reconstruct the crustal thickness of the ancient orogenic belt

and track the variation of crustal thickness. According to the following empirical formulas, we calculated the crustal thickness of the study area in the Early Cretaceous (Supplementary Table S6). The average crustal thickness obtained from the formula varies little about 34.7 km. In additions, combined with previous studies, we calculated the crustal thickness of the Langxian Early Cretaceous complex (~120 Ma, Wang et al. (2013)). Furthermore, Wang et al. (2013) proposed that the Early Cretaceous diorite in the Langxian area belongs to normal arc-type magmatic rock rather than adakite. The fractional crystallization of amphibole leads to the high Sr/Y values of the Langxian diorite in essence, and the petrogenesis of adakite-like features is not related to the crustal thickening. Therefore, we argue that the crustal thickness of the Early Cretaceous in Langxian area is about 33.7 km based on the empirical formula. The crustal thickness in Langxian area during the Cretaceous is consistent with the normal crustal thickness (~37 km) in Gangdese magmatic belt. This indicates that there was no significant crustal thickening in the Gangdese belt during the Early Cretaceous. The detailed empirical formulas are presented below:

$$\text{A). } H = 18.0505 \times \ln(3.3014 \times \text{Ce/Y}) \text{ (Mantle and Collins, 2008)}$$

$$\text{B). } H = 0.67 \times \text{Sr/Y} + 28.21 \text{ (Hu et al., 2017)}$$

Fundamentally, our calculated results are consistent with the Sr/Y and  $(\text{La/Yb})_N$  ratios, reflecting a plagioclase-dominated field rather than a garnet-dominated field. In conclusion, it is more appropriate to explain the Early Cretaceous magmatic activities in the Quesang area by the northward oblique subduction at a normal angle of the Neo-Tethys oceanic lithosphere. Moreover, we argue that the crustal thickening in the Gangdese belt may begin in the late Early Cretaceous.

## 6 Conclusion

- 1) Zircon U-Pb dating results show that the newly identified granitic pluton formed during the Aptian stage of the Early Cretaceous rather than the Oligocene, experiencing an incremental assembly process (crystallization age at circa 114–120 Ma).
- 2) According to the mineral TIMA surface scanning data, whole-rock geochemistry and zircon Lu-Hf isotopic compositions, the studied granitic pluton is characterized by arc-type features and ascribed to I-type granitic affinity.
- 3) The studied granitic pluton originated from partial melting of juvenile lower crust and minor ancient basement materials might participate in the magma evolution and formation as suggested by the Carboniferous inherited zircon and negative  $\epsilon_{\text{Hf}}(t)$  value.
- 4) The northward subduction angle of the Neo-Tethys oceanic slab may be normal, and there was no significant crustal thickening in the Gangdese region during the Early Cretaceous.
- 5) The granitic pluton shows a low magmatic oxygen fugacity similar to the Chile ore-barren granitoid rocks, suggesting a poor metallogenic potential.

## Data availability statement

The original contributions presented in the study are included in the article/Supplementary Material, further inquiries can be directed to the corresponding author.

## Author contributions

QW: investigation and writing; YM: investigation and editing and polishing; YW: Investigation and polishing; LJ: English polishing; ZW: Investigation and editing; GM: editing and polishing.

## Funding

National Natural Science Foundation of China (41902230). This study was co-supported by the Key Laboratory of Deep-Earth Dynamics of Ministry of Natural Resources (J1901-16), the National Natural Science Foundation of China (No. 41902230, 92055211), China-ASEAN Maritime Cooperation Fund Project (No. 12120100500017001) and the Young Innovative Projects of Shandong Province (2019KJH004).

## Acknowledgments

We are grateful to the reviewers for their constructive comments that improved the manuscript greatly. We thank editor for his efficient handling on this manuscript.

## Conflict of interest

The authors declare that the research was conducted in the absence of any commercial or financial relationships that could be construed as a potential conflict of interest.

## Publisher's note

All claims expressed in this article are solely those of the authors and do not necessarily represent those of their

affiliated organizations, or those of the publisher, the editors and the reviewers. Any product that may be evaluated in this article, or claim that may be made by its manufacturer, is not guaranteed or endorsed by the publisher.

## References

- Annen, C. (2011). Implications of Incremental Emplacement of Magma Bodies for Magma Differentiation, Thermal Aureole Dimensions and Plutonism-Volcanism Relationships. *Tectonophysics* 500, 3–10. doi:10.1016/j.tecto.2009.04.010
- Atherton, M. P., and Petford, N. (1993). Generation of Sodium-Rich Magmas from Newly Underplated Basaltic Crust. *Nature* 362 (6416), 144–146. doi:10.1038/362144a0
- Atherton, M. P., and Sanderson, L. M. (1985). “The Chemical Variation and Evolution of the Super-units of the Segmented Coastal Batholith,” in *Magmatism at a Plate Edge: The Peruvian Andes*. Editors Pitcher WS, M. P. Atherton, E. J. Cobbing, and R. D. Beckensale (Glasgow: Blackie), 208–227.
- Ballard, J. R., Palin, J. M., and Campbell, I. H. (2002). Relative Oxidation States of Magmas Inferred from Ce (IV)/Ce (III) in Zircon: Application to Porphyry Copper Deposits of Northern Chile. *Contrib. Mineral. Pet.* 144, 347–364. doi:10.1007/s00410-002-0402-5
- Cao, Y. H., Christina, Y. W., and Wei, B. (2019). Magma Oxygen Fugacity of Permian to Triassic Ni-Cu Sulfide-Bearing Mafic-Ultramafic Intrusions in the Central Asian Orogenic Belt, North China. *J. Asian Earth Sci.* 173, 250–262. doi:10.1016/j.jseae.2019.01.024
- Castro, A. (2020). The Dual Origin of I-type Granites: The Contribution from Experiments. *Geol. Soc. Spec. Publ.* 491 (1), 101–145. doi:10.1144/sp491-2018-110
- Chappell, B. W., and White, A. J. R. (1974). Two Contrasting Granite Types. *Pac. Geol.* 8, 173–174.
- Chen, W., Zhang, G. L., Ruan, M. F., Wang, S. A., and Xiong, X. L. (2021). Genesis of Intermediate and Silicic Arc Magmas Constrained by Nb/Ta Fractionation. *J. Geophys. Res. Solid Earth* 126 (3). doi:10.1029/2020jb020708
- Chen, Y., Zhu, D. C., Zhao, Z. D., Meng, F. Y., Wang, Q., Santosh, M., et al. (2014). Slab Breakoff Triggered ca.113Ma Magmatism Around Xainza Area of the Lhasa Terrane, Tibet. *Gondwana Res.* 26, 449–463. doi:10.1016/j.gr.2013.06.005
- Chu, M. F., Chung, S. L., Song, B., Liu, D., O'Reilly, S. Y., Pearson, N. J., et al. (2006). Zircon U-Pb and Hf Isotope Constraints on the Mesozoic Tectonics and Crustal Evolution of Southern Tibet. *Geol.* 34 (9), 745–748. doi:10.1130/g22725.1
- Chung, S. L., Chu, M. F., Zhang, Y. Q., Xie, Y., Lo, C. H., Lee, T. Y., et al. (2005). Tibetan Tectonic Evolution Inferred from Spatial and Temporal Variations in Post-collisional Magmatism. *Earth-Science Rev.* 68, 173–196. doi:10.1016/j.earscirev.2004.05.001
- Chung, S. L., Liu, D. Y., Ji, J. Q., Chu, M. F., Lee, H. Y., Wen, D. J., et al. (2003). Adakites from Continental Collision Zones: Melting of Thickened Lower Crust beneath Southern Tibet. *Geol.* 31 (11), 1021–1024. doi:10.1130/g19796.1
- Clemens, J. D., Stevens, G., and Farina, F. (2011). The Enigmatic Sources of I-type Granites: the Peritectic Connexion. *Lithos* 126, 174–181. doi:10.1016/j.lithos.2011.07.004
- Coleman, D. S., Gray, W., and Glazner, A. F. (2004). Rethinking the Emplacement and Evolution of Zoned Plutons: Geochronologic Evidence for Incremental Assembly of the Tuolumne Intrusive Suite, California. *Geol.* 32, 433–436. doi:10.1130/g20220.1
- Coulon, C., Maluski, H., Bollinger, C., and Wang, S. (1986). Mesozoic and Cenozoic Volcanic Rocks from Central and Southern Tibet: <sup>39</sup>Ar-<sup>40</sup>Ar Dating, Petrological Characteristics and Geodynamical Significance. *Earth Planet. Sci. Lett.* 79 (3–4), 281–302. doi:10.1016/0012-821x(86)90186-x
- Dai, J. G., Wang, C. S., Stern, R. J., Yang, K., and Shen, J. (2021). Forearc Magmatic Evolution during Subduction Initiation: Insights from an Early Cretaceous Tibetan Ophiolite and Comparison with the Izu-Bonin-Mariana Fore-Arc. *GSA Bull.* 133 (3–4), 753–776. doi:10.1130/b35644.1
- Debon, F., Le, Fort, P., Sheppard, S. M., and Sonet, J. (1986). The Four Plutonic Belts of the Transhimalaya-Himalaya: a Chemical, Mineralogical, Isotopic, and Chronological Synthesis along a Tibet-Nepal Section. *J. Petrology* 27, 219–250. doi:10.1093/ptrology/27.1.219
- Defant, M. J., and Drummond, M. S. (1990). Derivation of Some Modern Arc Magmas by Melting of Young Subducted Lithosphere. *Nature* 347 (6294), 662–665. doi:10.1038/347662a0
- Ding, L., Kapp, P., Zhong, D. L., and Deng, W. (2003). Cenozoic Volcanism in Tibet: Evidence for a Transition from Oceanic to Continental Subduction. *J. Petrology* 44 (10), 1833–1865. doi:10.1093/ptrology/egg061
- Dong, X., Zhang, Z. M., Geng, G. S., Liu, F., Wang, W., and Yu, F. (2010). Devonian Magmatism from the Southern Lhasa Terrane, Tibetan Plateau. *Acta Mineral. Sin.* 26 (7), 2226–2232.
- Ferry, J. M., and Watson, E. B. (2007). New Thermo Dynamic Models and Revised Calibrations for the Ti-In-Zircon and Zr-In-Rutile Thermometers. *Contrib. Mineral. Pet.* 154, 429–437. doi:10.1007/s00410-007-0201-0
- Gao, J. H., Zeng, L. S., Guo, C. L., Li, Q. L., and Wang, Y. Y. (2017). Late Cretaceous Tectonics and Magmatism in Gangdese Batholith, Southern Tibet: A Record from the Mafic-Dioritic-like Swarms within the Baidui Complex, Lhasa. *Acta Petrol. Sin.* 33 (8), 2412–2436.
- Ge, Y., Li, Y. L., Wang, X. N., Qian, X., Zhang, J., Zhou, A., et al. (2018). Oligocene-Miocene Burial and Exhumation of the Southernmost Gangdese Mountains from Sedimentary and Thermochronological Evidence. *Tectonophysics* 723, 68–80. doi:10.1016/j.tecto.2017.12.003
- Glazner, A. F., Bartley, J. M., Coleman, D. S., Gray, W., and Taylor, R. Z. (2004). Are Plutons Assembled over Millions of Years by Amalgamation from Small Magma Chambers? *GSA Today* 14, 4–11. doi:10.1130/1052-5173(2004)014<0004:apaomo>2.0.co;2
- Harris, N. B. W., Xu, R. H., Lewis, C. L., and Jin, C. W. (1988). Plutonic Rocks of the 1985 Tibet Geotraverse, Lhasa to Golmud. *Phil Trans. R. Soc Lond A327* (1594), 145–146.
- Hoskin, P. W. O., and Schaltegger, U. (2003). The Composition of Zircon and Igneous and Metamorphic Petrogenesis. *Rev. Mineralogy Geochem.* 53, 27–62. doi:10.2113/0530027
- Hou, Z. Q., Gao, Y. F., Qu, X. M., Rui, Z. Y., and Mo, X. X. (2004). Origin of Adakitic Intrusives Generated during Mid-miocene East-West Extension in Southern Tibet. *Earth Planet. Sci. Lett.* 220 (1–2), 139–155. doi:10.1016/s0012-821x(04)00007-x
- Hou, Z. Q., Yang, Z. M., Lu, Y. J., Kemp, A., Zheng, Y., Li, Q., et al. (2015). A Genetic Linkage between Subduction- and Collision-Related Porphyry Cu Deposits in Continental Collision Zones. *Geology* 43, 247–250. doi:10.1130/g36362.1
- Hrstka, T., Gottlieb, P., Skala, R., Breiter, K., and Motl, D. (2018). Automated Mineralogy and Petrology - Applications of TESCAN Integrated Mineral Analyzer (TIMA). *J. Geosci.* 63, 47–63. doi:10.3190/jgeosci.250
- Hu, F., Ducea, M. N., Liu, S., and Chapman, J. B. (2017). Quantifying Crustal Thickness in Continental Collisional Belts: Global Perspective and a Geologic Application. *Sci. Rep.* 7, 7058. doi:10.1038/s41598-017-07849-7
- Hu, Z. C., Liu, Y. S., Gao, S., Liu, W., Zhang, W., Tong, X., et al. (2012). Improved *In Situ* Hf Isotope Ratio Analysis of Zircon Using Newly Designed X Skimmer Cone and Jet Sample Cone in Combination with the Addition of Nitrogen by Laser Ablation Multiple Collector ICP-MS. *J. Anal. At. Spectrom.* 27, 1391–1399. doi:10.1039/c2ja30078h
- Huang, W., Liang, H., Zhang, J., Chen, X., Shuping, L., Zou, Y., et al. (2020). Formation of the Cretaceous Skarn Cu-Au Deposits of the Southern Gangdese Belt, Tibet: Case Studies of the Kelu and Sangbujiala Deposits. *Ore Geol. Rev.* 122, 103481. doi:10.1016/j.oregeorev.2020.103481
- Huang, Y., Zhao, Z. D., Zhu, D. C., Liu, Y., Liu, D., Zhou, Q., et al. (2017). The Geochronologic and Geochemical Constraints on the Early Cretaceous Subduction Magmatism in the Central Lhasa Subterranean, Tibet. *Geol. J.* 52, 463–475. doi:10.1002/gj.3112
- Irvine, T. N., and Baragar, W. R. A. (1971). A Guide to the Chemical Classification of the Common Volcanic Rocks. *Can. J. Earth Sci.* 8, 523–548. doi:10.1139/e71-055
- Ji, W. Q., Wu, F. Y., Liu, C. Z., and Chung, S. L. (2009a). Geochronology and Petrogenesis of Granitic Rocks in Gangdese Batholith, Southern Tibet. *Sci. China Ser. D-Earth. Sci.* 39 (7), 1240–1261. doi:10.1007/s11430-009-0131-y
- Ji, W. Q., Wu, F. Y., Chung, S. L., Li, J. X., and Liu, C. Z. (2009b). Zircon U-Pb Geochronology and Hf Isotopic Constraints on Petrogenesis of the Gangdese

## Supplementary material

The Supplementary Material for this article can be found online at: <https://www.frontiersin.org/articles/10.3389/feart.2022.979313/full#supplementary-material>

- Batholith, Southern Tibet. *Chem. Geol.* 262 (3-4), 229–245. doi:10.1016/j.chemgeo.2009.01.020
- Ji, W. Q., Wu, F. Y., Liu, X. C., Liu, Z. C., Zhang, C., Liu, T., et al. (2020). Pervasive Miocene Melting of Thickened Crust from the Lhasa Terrane to Himalaya, Southern Tibet and its Constraint on Generation of Himalayan Leuco Granite. *Geochimica Cosmochimica Acta* 278, 137–156. doi:10.1016/j.gca.2019.07.048
- Jiang, Z. Q., Wang, Q., Li, Z. X., Wyman, D. A., Tang, G. J., Jia, X. H., et al. (2012). Late Cretaceous (Ca. 90Ma) Adakitic Intrusive Rocks in the Kelu Area, Gangdese Belt (Southern Tibet): Slab Melting and Implications for Cu-Au Mineralization. *J. Asian Earth Sci.* 53, 67–81. doi:10.1016/j.jseas.2012.02.010
- Kapp, P., DeCelles, P. G., Leier, A. L., Fabijanic, J., He, S., Pullen, A., et al. (2007). The Gangdese Retroarc Thrust Belt Revealed. *GSA Today* 17 (7), 4–9. doi:10.1130/gsat01707a.1
- Kapp, P., and DeCelles, P. G. (2019). Mesozoic-Cenozoic Geological Evolution of the Himalayan-Tibetan Orogen and Working Tectonic Hypotheses. *Am. J. Sci.* 319, 159–254. doi:10.2475/03.2019.01
- Kapp, P., Murphy, M. A., Yin, A., Harrison, T. M., Ding, L., and Guo, J. (2003). Mesozoic and Cenozoic Tectonic Evolution of the Shiquanhe Area of Western Tibet. *Tectonics* 22 (4), 1029. doi:10.1029/2001tc001332
- Kapp, P., Yin, A., Harrison, T. M., and Ding, L. (2005). Cretaceous-Tertiary Shortening, Basin Development, and Volcanism in Central Tibet. *Geol. Soc. Am. Bull.* 117 (7), 865–878. doi:10.1130/b25595.1
- Kay, S. M., Ramos, V. A., and Marquez, M. (1993). Evidence in Cerro Pampavolcanic Rocks for Slab-Melting Prior to Ridge-Trench Collision in Southern South America. *J. Geol.* 101 (6), 703–714. doi:10.1086/648269
- Le, F. P., and Cronin, V. S. (1988). Granites in the Tectonic Evolution of the Himalaya, Karakoram and Southern Tibet. *Philosophical Trans. R. Soc. Lond. Ser. A* 326 (1589), 281–299.
- Leier, A. L., Kapp, P., Gehrels, G. E., and DeCelles, P. G. (2007). Detrital Zircon Geochronology of Carboniferous-Cretaceous Strata in the Lhasa Terrane, Southern Tibet. *Basin Res.* 19 (3), 361–378. doi:10.1111/j.1365-2117.2007.00330.x
- Li, G. X., Zeng, L. S., Gao, L. E., JiaHao, G., and LingHao, Z. (2021). Early Cretaceous Magmatism of the Langxian Complex in the Eastern Gangdese Batholith, Southern Tibet: Neo-Tethys Ocean Subduction Re-initiation. *Acta Petrol. Sin.* 37 (10), 2995–3034. doi:10.18654/1000-0569/2021.10.04
- Li, S., Calvin, F. M., Wang, T., Xiao, W., and Chew, D. (2022). Role of Sediment in Generating Contemporaneous, Diverse “Type” Granitoid Magmas. *Geology* 50 (4), 427–431. doi:10.1130/g49509.1
- Li, S. M., Wang, Q., Zhu, D. C., Stern, R. J., Cawood, P. A., Sui, Q., et al. (2018). One or Two Early Cretaceous Arc Systems in the Lhasa Terrane, Southern Tibet. *J. Geophys. Res. Solid Earth* 123, 3391–3413. doi:10.1002/2018jb015582
- Liang, Y. H., Chung, S. L., Liu, D. Y., Xu, Y., Wu, F. Y., Yang, J. H., et al. (2008). Detrital Zircon Evidence from Burma for Reorganization of the Eastern Himalayan River System. *Am. J. Sci.* 308 (4), 618–638. doi:10.2475/04.2008.08
- Liu, H., Li, G. M., Li, W. C., HanXiao, H., YouGuo, L., Yuan, O., et al. (2022). Petrogenesis and Tectonic Setting of the Late Early Cretaceous Kong Co A-type Granite in the Northern Margin of Central Lhasa Subterrane, Tibet. *Acta Petrol. Sin.* 38, 230–252. doi:10.18654/1000-0569/2022.01.15
- Loiselle, M. C., and Wones, D. R. (1979). Characteristics and Origin of an Orogenic Granites. *Geol. Soc. Am. Abstr. Programs* 11 (7), 468.
- Ma, L., Kerr, A. C., Wang, Q., Jiang, Z., Tang, G., Yang, J., et al. (2019a). Nature and Evolution of Crust in Southern Lhasa, Tibet: Transformation from Microcontinent to Juvenile Terrane. *J. Geophys. Res. Solid Earth* 124 (7), 6452–6474. doi:10.1029/2018jb017106
- Ma, L., Wang, Q., Kerr, A. C., Yang, J. H., Xia, X. P., Ou, Q., et al. (2017). Paleocene (c.62Ma) Leuco Granites in Southern Lhasa, Tibet: Products of Syn-Collisional Crustal Anatexis during Slab Roll-Back? *J. Petrology* 58, 2089–2114. doi:10.1093/petrology/egy001
- Ma, X. X., Meert, J. G., Xu, Z. Q., and Yi, Z. Y. (2018). Late Triassic Intra-oceanic Arc System within Neotethys: Evidence from Cumulate Appinite in the Gangdese Belt, Southern Tibet. *Lithosphere* 10 (4), 545–565. doi:10.1130/l682.1
- Ma, X. X., Xu, Z. Q., Liu, F., Zhao, Z. B., and Li, H. B. (2021). Continental Arc Tempos and Crustal Thickening: A Case Study in the Gangdese Arc, Southern Tibet. *Acta Geol. Sin.* 95, 107–123.
- Ma, X. X., Xu, Z. Q., and Meert, J. G. (2016). Eocene Slab Breakoff of Neotethys as Suggested by Dioritic Dykes in the Gangdese Magmatic Belt, Southern Tibet. *Lithos* 248–251, 55–65. doi:10.1016/j.lithos.2016.01.008
- Ma, X. X., Xu, Z. Q., Zhao, Z. B., and Yi, Z. Y. (2019b). Identification of a New Source for the Triassic Langxiexue Group: Evidence from a Gabbro-Diorite Complex in the Gangdese Magmatic Belt and Zircon Microstructures from Sandstones in the Tethyan Himalaya. *South. Tibet. Geosph.* 16, 1–28.
- Ma, X. X., Xu, Z. Q., Zhao, Z. B., and Yi, Z. Y. (2020). Identification of a New Source for the Triassic Langxiexue Group: Evidence from a Gabbro-Diorite Complex in the Gangdese Magmatic Belt and Zircon Microstructures from Sandstones in the Tethyan Himalaya, Southern Tibet. *Geosphere* 16 (1), 407–434. doi:10.1130/ges02154.1
- Maniar, P. D., and Piccoli, P. M. (1989). Tectonic Discrimination of Granitoids. *Geol. Soc. Am. Bull.* 101, 635–643. doi:10.1130/0016-7606(1989)101<0635:tdog>2.3.co;2
- Mantle, G. W., and Collins, W. J. (2008). Quantifying Crustal Thickness Variations in Evolving Orogens: Correlation between Arc Basalt Composition and Moho Depth. *Geol.* 36, 87–90. doi:10.1130/g24095a.1
- McDonough, W. F. (2003). “Compositional Model for the Earth’s Core,” in *The Mantle and Core, Treatise on Geochemistry*, 2. Editor R. W. Carlson (Amsterdam: Elsevier), 547–568.
- Meng, Y. K., Mooney, W. D., Ma, Y., Xu, H., and Tang, R. (2019). Back-arc Basin Evolution in the Southern Lhasa Sub-terrane, Southern Tibet: Constraints from U-Pb Ages and *In-Situ* Lu-Hf Isotopes of Detrital Zircons. *J. Asian Earth Sci.* 185, 104026. doi:10.1016/j.jseas.2019.10.4026
- Meng, Y. K., Santosh, M., Mao, G. Z., Lin, P., Liu, J., and Ren, P. (2020). New Constraints on the Tectono-Magmatic Evolution of the Central Gangdese Belt from Late Cretaceous Magmatic Suite in Southern Tibet. *Gondwana Res.* 80, 123–141. doi:10.1016/j.gr.2019.10.014
- Meng, Y. K., Wang, Q. L., Wang, X., Chen, X., Yuan, H., and Meng, F. (2021). Late Mesozoic Diorites of the Middle Gangdese Magmatic Belt of Southern Tibet: New Insights from SHRIMP U-Pb Dating and Sr-Nd-Hf-O Isotopes. *Lithos* 404–405, 106420. doi:10.1016/j.lithos.2021.106420
- Meng, Y. K., Xu, Z. Q., Gao, C. S., Xu, Y., and Liu, R. H. (2018). The Identification of the Eocene Magmatism and Tectonic Significance in the Middle Gangdese Magmatic Belt, Southern Tibet. *Acta Petrol. Sin.* 34 (3), 513–546.
- Meng, Y. K., Xu, Z. Q., Santosh, M., Ma, X., Chen, X., Guo, G., et al. (2016). Late Triassic Crustal Growth in Southern Tibet: Evidence from the Gangdese Magmatic Belt. *Gondwana Res.* 37, 449–464. doi:10.1016/j.gr.2015.10.007
- Meng, Y. K., Yuan, H. Q., Wei, Y. Q., Zhang, S. K., and Liu, J. Q. (2022). Research Progress and Prospect of the Gangdese Magmatic Belt in Southern Tibet. *Geol. J. China Univ.* 28, 1–31.
- Middlemost, E. A. K. (1994). Naming Materials in the Magma/Igneous Rock System. *Earth. Sci. Rev.* 37, 215–224. doi:10.1016/0012-8252(94)90029-9
- Mo, X. X., Dong, G. C., Zhao, Z. D., Zhu, D., Zhou, S., and Niu, Y. (2009). Mantle Input to the Crust in Southern Gangdese, Tibet, during the Cenozoic: Zircon Hf Isotopic Evidence. *J. Earth Sci.* 20, 241–249. doi:10.1007/s12583-009-0023-2
- Mo, X. X., Hou, Z. Q., Niu, Y. L., Dong, G., Qu, X., Zhao, Z., et al. (2007). Mantle Contributions to Crustal Thickening during Continental Collision: Evidence from Cenozoic Igneous Rocks in Southern Tibet. *Lithos* 96 (1-2), 225–242. doi:10.1016/j.lithos.2006.10.005
- Mo, X. X., Niu, Y. L., Dong, G. C., Zhao, Z., Hou, Z., Zhou, S., et al. (2008). Contribution of Syn-collisional Felsic Magmatism to Continental Crust Growth: A Case Study of the Paleogene Linzizong Volcanic Succession in Southern Tibet. *Chem. Geol.* 250 (1-4), 49–67. doi:10.1016/j.chemgeo.2008.02.003
- PatinoDouce, A. E. (1999). What Do Experiments Tell Us about the Relative Contributions of Crust and Mantle to the Origin of Granitic Magmas? *Geol. Soc. Lond. Spec. Publ.* 168, 55–75.
- Pearce, J. A., Stern, R. J., Bloomer, S. H., and Fryer, P. (2005). Geochemical Mapping of the Mariana Arc-Basin System: Implications for the Nature and Distribution of Subduction Components. *Geochem. Geophys. Geosyst.* 6 (7), Q07006. doi:10.1029/2004gc000895
- Peccerillo, A., and Taylor, S. R. (1976). Geochemistry of Eocene Calc-Alkaline Volcanic Rocks from the Kastamonu Area, Northern Turkey. *Contr. Mineral. Pet.* 58, 63–81. doi:10.1007/bf00384745
- Pitcher, W. S. (1983). “Granite Type and Tectonic Environment,” in *Mountain Building Process*. Editor K. Hsu (London: Academic Press).
- Quidelleur, X., Grove, M., Lovera, O. M., Harrison, T. M., Yin, A., and Ryerson, F. J. (1997). Thermal Evolution and Slip History of the Renbu Zedong Thrust, Southeastern Tibet. *J. Geophys. Res.* 102 (B2), 2659–2680. doi:10.1029/96jd02483
- Rapp, R. P., and Watson, E. B. (1995). Dehydration Melting of Meta-Basalt at 8–32kbar: Implications for Continental Growth and Crust-Mantle Recycling. *J. Petrology* 36, 891–931. doi:10.1093/petrology/36.4.891
- Rogers, G., and Hawkesworth, C. J. (1989). A Geochemical Traverse across the North Chilean Andes: Evidence for Crust Generation from the Mantle Wedge. *Earth Planet. Sci. Lett.* 91 (3-4), 271–285. doi:10.1016/0012-821x(89)90003-4
- Sajona, F. G., Maury, R. C., Bellon, H., Cotton, J., and Defant, M. (1996). High Field Strength Element Enrichment of Pliocene-Pleistocene Island Arc Basalts,

- Zamboanga Peninsula, Western Mindanao (Philippines). *J. Petrol.* 37 (3), 693–726. doi:10.1093/ptrology/37.3.693
- Scharer, U., Xu, R. H., and Allegre, C. J. (1984). UPb Geochronology of Gangdese (Transhimalaya) Plutonism in the Lhasa-Xigaze Region, Tibet. *Earth Planet. Sci. Lett.* 69, 311–320. doi:10.1016/0012-821x(84)90190-0
- Sun, S. S., and McDonough, W. F. (1989). Chemical and Isotopic Systematics of Oceanic Basalts: Implications for Mantle Composition and Processes. *Geol. Soc. Lond., Spec. Publ.* 42, 313–345. doi:10.1144/gsl.sp.1989.042.01.19
- Trail, D., Bruce Watson, E., and Tailby, N. D. (2012). Ce and Eu Anomalies in Zircon as Proxies for the Oxidation State of Magmas. *Geochim. Cosmochim. Acta* 97, 70–87. doi:10.1016/j.gca.2012.08.032
- Wang, C., Ding, L., Zhang, L. Y., Kapp, P., Pullen, A., and Yue, Y. H. (2016). Petrogenesis of Middle-Late Triassic Volcanic Rocks from the Gangdese Belt, Southern Lhasa Terrane: Implications for Early Subduction of Neo-Tethyan Oceanic Lithosphere. *Lithos* 262, 320–333. doi:10.1016/j.lithos.2016.07.021
- Wang, H. T., Zeng, L. S., Xu, C. P., JiaHao, G., LingHao, Z., YaFei, W., et al. (2020). Petrogenesis and Geodynamic Significances of Late Jurassic-Cretaceous Intrusion in the Mainling Area, Eastern Gangdese, Southern Tibet. *Acta Petrol. Sin.* 36 (10), 3041–3062. doi:10.11865/1000-0569/2020.10.07
- Wang, L. X., Xu, D. R., Chen, G. W., and Zhu, Y. (2017). Chronology and Genesis of S-type Granites in Hetai District, Guangdong Province: Constraints from LA-ICP-MS Zircon U-Pb Dating and Tourmaline Boron Isotope *In-Situ* Analyses. *Acta Geol. Sin. - Engl. Ed.* 91, 96–97. doi:10.1111/1755-6724.13203
- Wang, L., Zeng, L. S., Gao, L. E., and Chen, Z. Y. (2013). Control of Bursting Behavior in Neurons by Autaptic Modulation. *Neuro. Sci.* 29 (6), 1977–1984. doi:10.1007/s10072-013-1429-2
- Wang, T., Wang, X. X., Guo, L., Zhang, L., Tong, Y., and Li, S. (2017). Granitoid and Tectonics. *Acta Petrol. Sin.* 33 (5), 1459–1478.
- Wei, B., Christina, Y. W., Yann, L., Xie, L., and Cao, Y. (2019). S and C Isotope Constraints for Mantle-Derived Sulfur Source and Organic Carbon-Induced Sulfide Saturation of Magmatic Ni-Cu Sulfide Deposits in the Central Asian Orogenic Belt, North China. *Econ. Geol.* 144, 787–806. doi:10.5382/econgeo.4652
- Wen, D. R., Chung, S. L., Song, B., Iizuka, Y., Yang, H. J., Ji, J., Lu, Z. Y., Su, X., and Li, C. Z. (2008b). Late Cretaceous Gangdese Intrusions of Adakitic Geochemical Characteristics, SE Tibet: Petrogenesis and Tectonic Implications. *Lithos* 105 (1-2), 1–11. doi:10.1016/j.lithos.2008.02.005
- Wen, D. R., Liu, D. Y., Chung, S. L., Chu, M., Ji, J., Zhang, Q., et al. (2008a). Zircon SHRIMP U-Pb Ages of the Gangdese Batholith and Implications for Neotethyan Subduction in Southern Tibet. *Chem. Geol.* 252, 191–201. doi:10.1016/j.chemgeo.2008.03.003
- Wright, J. B. (1969). A Simple Alkalinity Ratio and its Application to Questions of Non-orogenic Granite Genesis. *Geol. Mag.* 106, 370–384. doi:10.1017/s0016756800058222
- Wu, F. Y., Ji, W. Q., Liu, C. Z., and Chung, S. L. (2010). Detrital Zircon U-Pb and Hf Isotopic Data from the Xigaze Fore-Arc Basin: Constraints on Transhimalayan Magmatic Evolution in Southern Tibet. *Chem. Geol.* 271 (1-1), 13–25. doi:10.1016/j.chemgeo.2009.12.007
- Wu, F. Y., Li, X. H., and Zheng, Y. F. (2007). Discussions on the Petrogenesis of Granites. *Acta Petrol. Sin.* 23 (6), 1217–1238.
- Wu, F. Y., Liu, X. C., Ji, W. Q., Wang, J., and Yang, L. (2017). Highly Fractionated Granites: Recognition and Research. *Sci. China Earth Sci.* 60, 1201–1219. doi:10.1007/s11430-016-5139-1
- Wu, W. Z., and Wang, J. G. (2020). Oxygen Fugacity Characteristics of Monzonitic Granites in the Middle Late Cretaceous in Sangye Area, Tibet. *J. Hebei Geo Univ.* 4, 6–11.
- Xu, Q., Zeng, L. S., Gao, J. H., LingHao, Z., YaFei, W., and ZhaoPing, H. (2019). Geochemical Characteristics and Genesis of the Songka Late Cretaceous Adakitic High-Mg Diorite in the Southern Margin of Gangdese, Southern Tibet. *Acta Petrol. Sin.* 35 (2), 455–471. doi:10.11865/1000-0569/2019.02.12
- Yin, A., and Harrison, T. M. (2000). Geologic Evolution of the Himalayan-Tibetan Orogen. *Annu. Rev. Earth Planet. Sci.* 28, 211–280. doi:10.1146/annurev.earth.28.1.211
- Zeng, L. S., Gao, L. E., Guo, C. L., Hou, K. J., and Wang, Q. (2017). Early Cretaceous Forearc Extension of the Gangdese Continental Arc, Southern Tibet. *Acta Petrol. Sin.* 33 (8), 2377–2394.
- Zhang, C. C., Sun, W. D., Wang, J. T., Zhang, L. p., Sun, S. j., and Wu, K. (2017). Oxygen Fugacity and Porphyry Mineralization: a Zircon Perspective of Dexing Porphyry Cu Deposit, China. *Geochim. Cosmochim. Acta* 206, 343–363. doi:10.1016/j.gca.2017.03.013
- Zhang, H. L., Yang, W. G., Zhu, L. D., Lu, Z. Y., Su, X., and Li, C. Z. (2019b). Zircon U-Pb Age, Geochemical Characteristics and Geological Significance of Highly Differentiated S-type Granites in the South Lhasa Block. *Mineralogy Petrology* 39 (01), 52–62.
- Zhang, K. J., Xia, B. D., Wang, G. M., Li, Y. T., and Ye, H. F. (2004). Early Cretaceous Stratigraphy, Depositional Environments, Sandstone Provenance, and Tectonic Setting of Central Tibet, Western China. *Geol. Soc. Am. Bull.* 116, 1202–1222. doi:10.1130/b25388.1
- Zhang, L. P., Hu, Y. B., Deng, J. H., Wang, J., Wang, K., Sui, Q., et al. (2021a). Genesis and Mineralization Potential of the Late Cretaceous Chemen Granodioritic Intrusion in the Southern Gangdese Magmatic Belt, Tibet. *J. Asian Earth Sci.* 217, 104829. doi:10.1016/j.jseas.2021.104829
- Zhang, Y. Z., Wang, X. L., Li, J. Y., He, Z. Y., Zhang, F. F., Chen, X., et al. (2021b). Oligocene Leuco Granites of the Gangdese Batholith, Southern Tibet: Fractional Crystallization of Felsic Melts from Juvenile Lower Crust. *J. Petrology* 62, 1–27. doi:10.1093/ptrology/egab076
- Zhang, Z. M., Ding, H. X., Dong, X., and ZuoLin, T. (2019a). Formation and Evolution of the Gangdese Magmatic Arc, Southern Tibet. *Acta Petrol. Sin.* 35, 275–294. doi:10.11865/1000-0569/2019.02.01
- Zhang, Z. M., Ding, H. X., Palin, R. M., Dong, X., Tian, Z., and Chen, Y. (2020). The Lower Crust of the Gangdese Magmatic Arc, Southern Tibet, Implication for the Growth of Continental Crust. *Gondwana Res.* 77, 136–146. doi:10.1016/j.gr.2019.07.010
- Zhang, Z. M., Dong, X., Liu, F., Lin, Y. H., Yan, R., and Santosh, M. (2012). Tectonic Evolution of the Amdo Terrane, Central Tibet: Petrochemistry and Zircon U-Pb Geochronology. *J. Geol.* 120 (4), 431–451. doi:10.1086/665799
- Zhao, S. J., Zhao, Z. D., Tang, Y., NingYuan, Q., Dong, L., Wang, Q., et al. (2021). Geochemistry and Petrogenesis of Jurassic Granites in Nyemo Area, South Lhasa Terrane, Tibet. *Acta Petrol. Sin.* 37 (11), 3464–3478. doi:10.11865/1000-0569/2021.11.13
- Zhao, Z., Hu, D., Wu, Z., and Lu, L. (2012). Molybdenite Re-os Isotopic Dating of Sangbujiala Copper Deposit in the South Margin of the Eastern Gangdese Section, Tibet, and its Geological Implications. *J. Geomech.* 18, 178–186.
- Zhu, D. C., Mo, X. X., Niu, Y. L., Zhao, Z. D., Wang, L. Q., Liu, Y. S., et al. (2009b). Geochemical Investigation of Early Cretaceous Igneous Rocks along an East-West Traverse throughout the Central Lhasa Terrane, Tibet. *Chem. Geol.* 268 (3-4), 298–312. doi:10.1016/j.chemgeo.2009.09.008
- Zhu, D. C., Wang, Q., Cawood, P. A., Zhao, Z., and Mo, X. (2017). Raising the Gangdese Mountains in Southern Tibet. *J. Geophys. Res. Solid Earth* 122 (1), 214–223. doi:10.1002/2016jb013508
- Zhu, D. C., Wang, Q., Chung, S. L., Cawood, P. A., and Zhao, Z. D. (2019). Gangdese Magmatism in Southern Tibet and India-Asia Convergence since 120 Ma. *Geol. Soc. Lond. Spec. Publ.* 483, 583–604. doi:10.1144/sp483.14
- Zhu, D. C., Zhao, Z. D., Niu, Y., Dilek, Y., Hou, Z. Q., and Mo, X. X. (2013). The Origin and Pre-cenozoic Evolution of the Tibetan Plateau. *Gondwana Res.* 23, 1429–1454. doi:10.1016/j.gr.2012.02.002
- Zhu, D. C., Zhao, Z. D., Niu, Y. L., Dilek, Y., Wang, Q., Ji, W. H., et al. (2012). Cambrian Bimodal Volcanism in the Lhasa Terrane, Southern Tibet: Record of an Early Paleozoic Andean-type Magmatic Arc in the Australian Proto-Tethyan Margin. *Chem. Geol.* 328, 290–308. doi:10.1016/j.chemgeo.2011.12.024
- Zhu, D. C., Zhao, Z. D., Niu, Y. L., Mo, X. X., Chung, S. L., Hou, Z. Q., et al. (2011). The Lhasa Terrane: Record of a Microcontinent and its Histories of Drift and Growth. *Earth Planet. Sci. Lett.* 301 (1-2), 241–255. doi:10.1016/j.epsl.2010.11.005
- Zhu, D. C., Zhao, Z. D., Pan, G. T., Lee, H. Y., Kang, Z. Q., Liao, Z. L., et al. (2009a). Early Cretaceous Subduction Related Adakite-like Rocks of the Gangdese Belt, Southern Tibet: Products of Slab Melting and Subsequent Melt-Peridotite Interaction? *J. Asian Earth Sci.* 34 (3), 298–309. doi:10.1016/j.jseas.2008.05.003
- Zong, K. Q., Klemd, R., Yuan, Y., He, Z., Guo, J., Shi, X., et al. (2017). The Assembly of Rodinia: The Correlation of Early Neoproterozoic (Ca. 900 Ma) High-Grade Metamorphism and Continental Arc Formation in the Southern Beishan Orogen, Southern Central Asian Orogenic Belt (CAOB). *Precambrian Res.* 290, 32–48. doi:10.1016/j.precamres.2016.12.010